Chapter 8

Models of Accommodation

George K. Hung[1], Kenneth J. Ciuffreda[2], Madjid Khosroyani[3], Bai-Chuan Jiang[4]

[1] *Dept. of Biomedical Engineering, Rutgers University, 617 Bowser Rd., Piscataway, NJ 08854-8014, PH: (732) 445-4137, FX: (732) 445-3753, EM: shoane@rci.rutgers.edu*

[2] *Dept. of Vision Sciences, State University of New York, State College of Optometry, 33 West 42nd St. New York, NY 10036; PH: (212) 780-5132, FX: (212) 780-5124; EM: kciuffreda@sunyopt.edu*

[3] *Tarbiat Modarres University, P. O. Box 14155-4838, Tehran, Iran; EM: khosro_m@net1cs.modarres.ac.ir*

[4] *College of Optometry, Health Professions Division, Nova Southeastern University, 3200 South University Dr., Ft. Lauderdale, FL 33328, PH: (954) 262-1444, FX: (954) 262-1818, EM: bjiang@nova.edu*

8.1 INTRODUCTION

The ability to see clearly at different distances is one of the most important functions of the human visual system. This is performed routinely and effortlessly in daily life by the process called accommodation. During this process, the accommodation system must sense that a new target is defocused beyond a blur threshold, develop the appropriate neurological control signal based on blur magnitude, and then adjust relatively rapidly the optics of the eye via the ciliary muscle until the target is once again in focus. Thus, it involves feedback regulation of visual optics via the sensing of retinal image blur. In addition, since blur per se does not provide the light vergence direction (Stark, 1968), the accommodation system must use perceptual cues and other sources of information to determine the appropriate direction of focus (Ciuffreda, 1991, 1998). It does this remarkably well, so that rarely does accommodation occur in the wrong direction under natural viewing conditions. Moreover, accommodation

takes place repeated in daily life, so that the system must be continually available to provide clear vision in the performance of a variety of tasks at a range of different distances.

Helmholtz (1855) was the first to elucidate the ocular changes during accommodation. The basic structures involved are shown in Fig. 8.1a. The only active element in this process is the ciliary muscle, whereas all other elements act in a passive manner. During increased accommodation driven by parasympathetic innervation (Kaufman, 1992; Fig. 8.1b), the ciliary muscle contracts, which causes it to shift forward and inward, as well as stretch the choroid and posterior zonules (Ciuffreda, 1991, 1998). In this process, the tension in the anterior zonules is reduced, thus relaxing the inherent forces of the elastic lens capsule, and returning the lens to its more natural rounded shape (Fig. 8.1b). This increases the optical power of the crystalline lens to focus the near target's image on the retina. On the other hand, during a decrease in accommodation, the ciliary muscle reduces its state of contraction, and the passive restoring forces of the spring-like choroid and posterior zonules return each element towards its former position. The tension on the anterior zonules is now increased, thus pulling on the capsule and lens centrifugally, thereby causing the front surface of the lens to flatten (Fig. 8.1b). This decreases the optical power of the crystalline lens to focus a distant target's image on the retina.

Higher cortical centers are involved in accommodation. Briefly, the summated blur signals are transmitted through the magnocellular layer of the lateral geniculate nucleus to arrive at area 17 of the visual cortex (Moses, 1981; Ciuffreda, 1991, 1998). The summated cortical cell responses form a sensory blur signal. The signal is then transmitted to the parietal-temporal areas for processing and dissemination (Jampel, 1959; Harrison, 1987; Ohsuka et al, 1988). This supranuclear signal then goes on to the midbrain Edinger-Westphal nucleus, where the motor command is formulated (Gamlin, 1999). The motor command is transmitted to the ciliary muscle via the oculomotor (III) nerve, the ciliary ganglion, and then the short ciliary nerve (Warwick, 1954). This causes a change in the state of contraction of the ciliary muscle, which in turn deforms the crystalline lens to attain a clear and in-focus retinal image of the target.

However, nearly 150 years after Helmholtz (1855), accommodation was still being discussed in qualitative or descriptive terms only. For example, Heath (1956a) divided and categorized accommodation into four components: reflex (blur), convergence, proximity, and tonic. These are important aspects of accommodation, but they remained as isolated components that had not been linked together in a systematic manner. Such

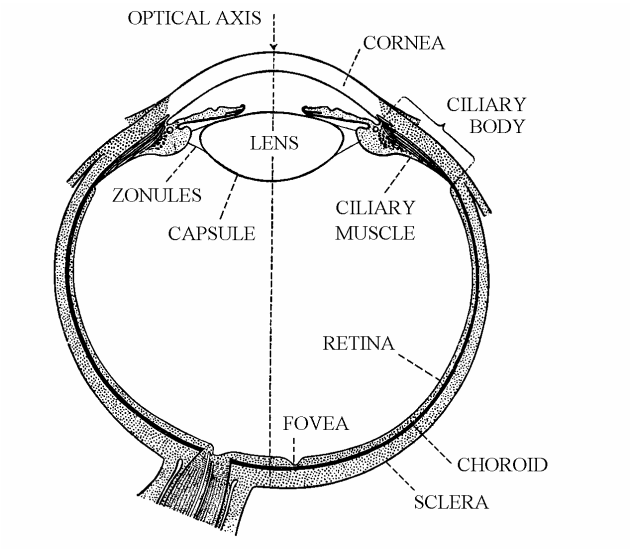

Fig. 8.1a.

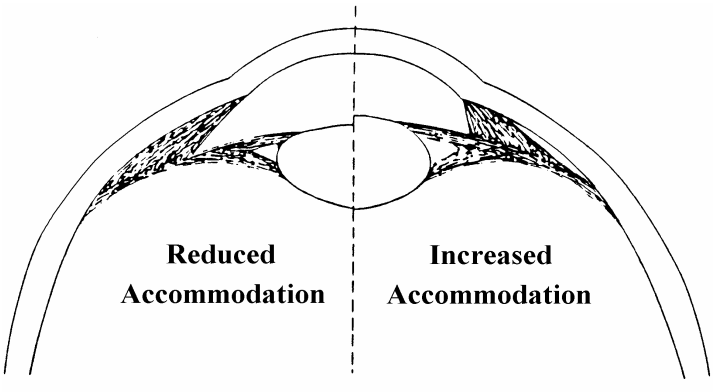

Fig. 8.1b.

Figure 8.1. (a) Horizontal section of the eye showing the major ocular components for accommodation. Adapted from Last (1968), pg. 30, Fig. 21, with permission of Kluwer Academic/Plenum Publishers. (b) Split view of the eye showing (left) relatively flat lens front surface curvature associated with reduced accommodation, and (right) relatively steep front surface curvature associated with increased accommodation. Adapted from Ciuffreda (1998), pg. 78, Fig. 4-1A, with permission of Harcourt Health Sciences.

conceptualization of these components is essential because, as noted above, accommodation involves an interactive feedback process. Yet, it is unclear, based on the descriptions of the components, how they would interact within a feedback loop. Moreover, a descriptive analysis of such component interactions would be very cumbersome and imprecise. Hence, a method was needed to quantify these individual elements and their feedback interactions in a more compact, precise, and unifying manner. Such a technique, called control systems theory, was first used qualitatively by Westheimer (1963) for the accommodation and vergence systems, and was also more formally introduced mathematically for the accommodation system by Stark and others (Stark and Takahashi, 1962; Stark et al, 1962). The use of control systems theory provided a new and powerful tool in the investigation of the accommodation system by allowing the development of homeomorphic and physiologically-realistic representations of the various components of the accommodation system, as well as the quantification of their feedback interactions. A number of models have been proposed since the 1960's, with each model advancing our understanding of the intricate and elegant process of accommodation.

These models have attempted to address two important issues: (1) How does the accommodation system use retina-image defocus, which provides an even-error signal that contains blur magnitude but not direction information, to accommodate in the appropriate direction?, and (2) Is the accommodation system governed by continuous or discrete feedback control?

In this chapter, we will first present some basic static and dynamic accommodative response information. Then, many of the earlier models of accommodation will be presented, and each model's configuration and applicability will be critically discussed. Finally, we will present our recent static and dynamic models which capture the most important characteristics of the accommodation system, and furthermore provide answers to the two major questions posed above.

8.2 BASIC PROPERTIES OF ACCOMMODATION

8.2.1 Static Behavior

The basic static property of the accommodation system can be seen in a plot of accommodative response (AR) versus accommodative stimulus (AS) (Ciuffreda and Kenyon, 1983; Fig. 8.2). This can be obtained by varying target distance from far to near in increments of diopters (D, a unit of optical power equal to the reciprocal of the distance of the target from the observer in meters) and measuring the steady-state accommodative response at each AS level. Inspection of Fig. 8.2 shows that the accommodative stimulus-response (AS/R) function does not fall on the 1:1 line, and moreover is not a simple linear function. Instead, the response can be divided into at least four zones (Ciuffreda and Kenyon, 1983; Ciuffreda, 1991, 1998). (1) The initial non-linear portion of the curve from 0 to 1.5 D of AS over which the AR is approximately constant; (2) the linear manifest zone over which a change in AS produces a proportional change in AR; this response is typically less than the stimulus, producing the so-called "lazy lag of accommodation" (Morgan, 1968); (3) the nonlinear transition zone (region of soft saturation)

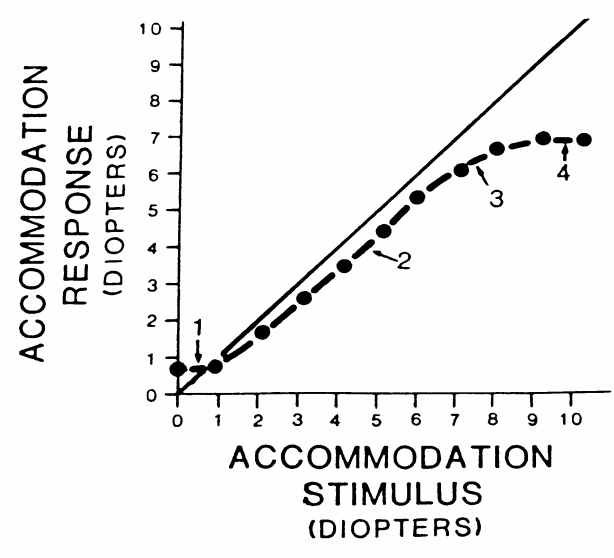

Figure 8.2. Schematic plot of the accommodative stimulus-response function. Equivalence of accommodative stimulus and response is represented by the diagonal (1:1) line. Reprinted from Ciuffreda and Kenyon (1983), pg. 102, Fig. 5.1, with permission of K. J. Ciuffreda, the copyright holder.

over which further increases in the stimulus produce a change in response, but progressively smaller than would be found for the same stimulus change over the manifest zone; and (4) the nonlinear latent zone (region of hard saturation), which defines the amplitude of accommodation, over which still further increases in the accommodative stimulus fails to produce additional increases in the lens response; however, ciliary body force can still increase in this zone, but the biomechanics of the overall accommodation system impedes further rounding of the lens to increase lenticular dioptric power; thus, functional presbyopia is attained (Saladin and Stark, 1975).

8.2.2 Dynamic behavior

Accommodative responses to pulse, step, and ramp stimuli are presented in Fig. 8.3a-c, respectively (Campbell and Westheimer, 1960). The pulse response (Fig. 8.3a) follows the pulse stimulus after a delay, and it has a duration approximately equal to that of the stimulus. This has been cited as evidence for continuous processing in the accommodation system (Campbell and Westheimer, 1960). However, as discussed in Section 8.5, a non-continuous process that responds to rapid changes in the stimulus could also account for the accommodative behavior (Hung et al, 1986; Khosroyani, 2000). The step response (Fig. 8.3b) typically exhibits a latency of 350-400 msec and an exponential rise with a time constant of about 250 msec (Campbell and Westheimer, 1960; Stark et al, 1965; Tucker and Charman, 1979; Krishnan and Stark, 1975). The ramp response (Fig. 8.3c) shows small wavering movements both for its rising and falling portions. A more systematic study using ramp stimuli of various velocities (Fig. 8.4; Hung and Ciuffreda, 1988) found dynamic characteristics that were contingent upon the stimulus ramp velocity. For relatively slow ramps (0.5 D/sec), the responses followed the target reasonably well. On the other, for intermediate velocities (1 to 2 D/sec), the responses consisted of mutiple-step movements in which the end of the step approximately coincided with the instantaneous position of the target. Further, for higher velocities ($\geq$ 3 D/sec), the responses consisted primarily of steps and step-ramps. These results indicated that the accommodation system behaved differently based on the target velocity, and furthermore suggested a two-part or dual-mode control process consisting of open- and closed-loop components (see Sub-Section 8.4.2 Fig. 8.23, for details). Sinusoidal responses to various temporal frequencies exhibit a decrease in response amplitude and increase in phase lag with increasing stimulus frequency (Fig. 8.5) (Kasai et al, 1971; Fujii et al, 1970).

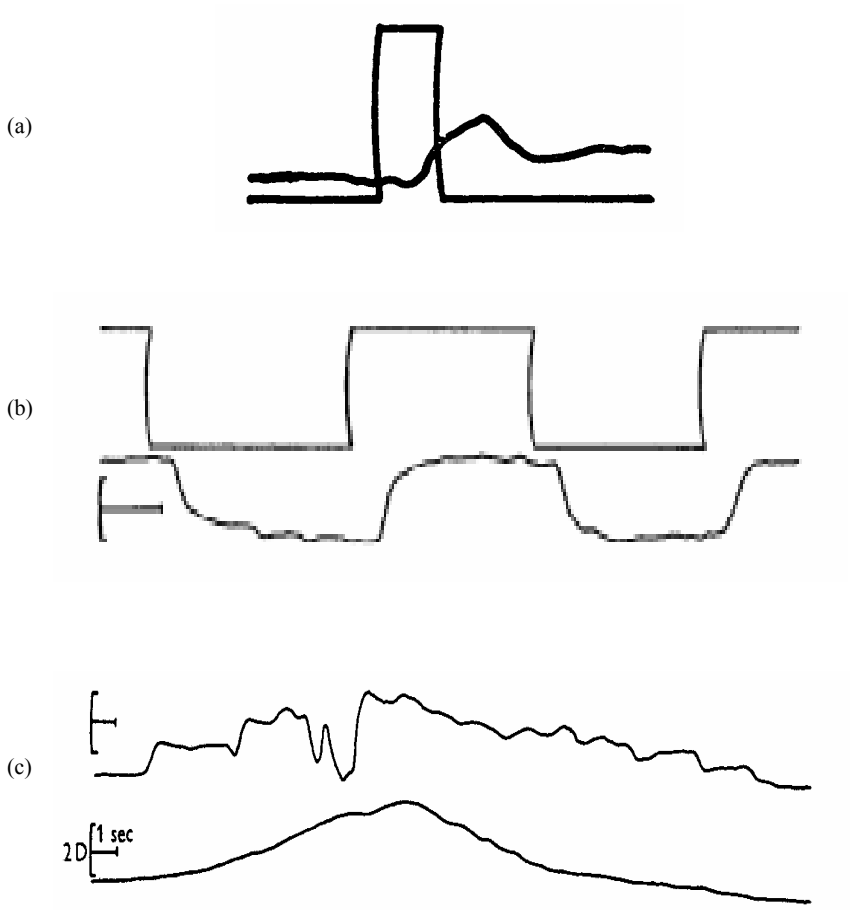

Fig. 8.3. Accommodative responses to: (a) 2 D pulse stimulus of 0.32 sec duration; (b) 2 D step and return to zero level of accommodation stimulus. Marker length: horizontal - 1sec; vertical - 1D; (c) gradually-changing stimulus, similar to an up- and then down-ramp stimulus. Note the irregular bumpy responses to the smoothly changing ramp stimulus. For a-c, response on top and stimulus on bottom. Reprinted with from Campbell and Westheimer (1959), pp. 288, 291, 294, Figs. 3, 7, 10, with permission of The Physiological Society.

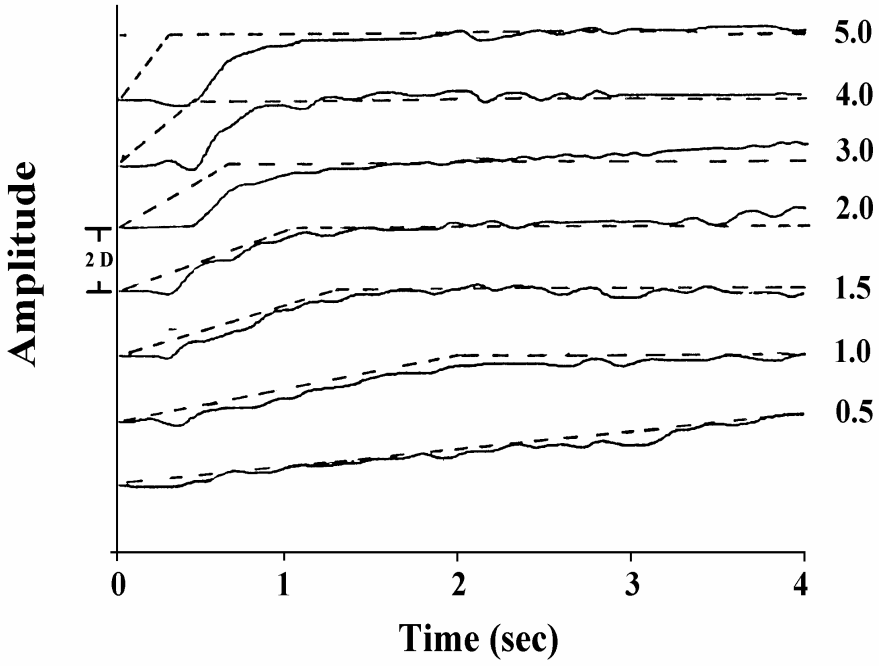

Figure 8.4. Accommodative responses (solid) to different ramp stimuli (dashed) with velocities (shown at right of curve) ranging from 0.5 to 5.0 D/sec. Maximum stimulus amplitude is 2D. Subj. GH. Note the multiple-steps in the responses to 1.0, 1.5 and 2.0 D/sec ramps, and progressive shift from step-ramp to step responses for the 3.0, 4.0 and 5.0 D/sec ramp stimuli. Reprinted from Hung and Ciuffreda (1988), pg. 330, Fig. 5, with permission of Elsevier Science.

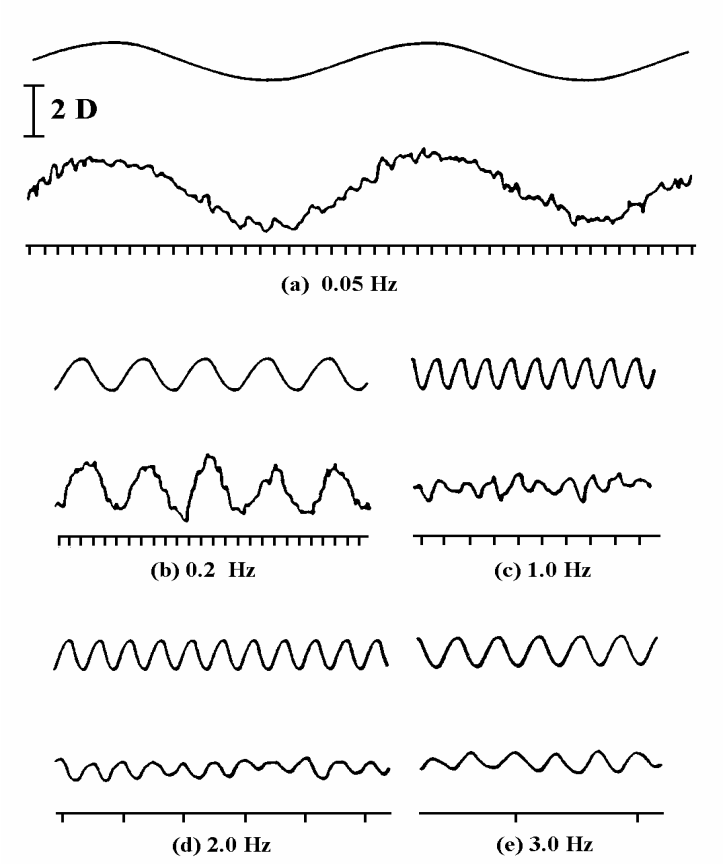

Figure 8.5. Accommodative responses to sinusoidal stimuli at various temporal frequencies. In each case, the upper record shows the stimulus change, the middle trace the corresponding response, and the bottom line is marked in seconds. Reprinted from Kasai et al (1971), pg. 569, with permission of Osaka University.

8.3 PREVIOUS MODELS OF ACCOMMODATION

Early models had some success in describing the behavior of the accommodation system. The following models are presented based on a conceptually progressive rather than historical sequence.

8.3.1 Westheimer model

Westheimer (1963) proposed a descriptive feedback model for accommodation showing the focus error (i.e., the difference between dioptric target distance and the accommodative response) driving the accommodation center (Fig. 8.6). This in turn is input to the peripheral mechanism, or plant, to generate the accommodative response. A similar feedback loop for vergence is also shown. Based on optical and pharmacological

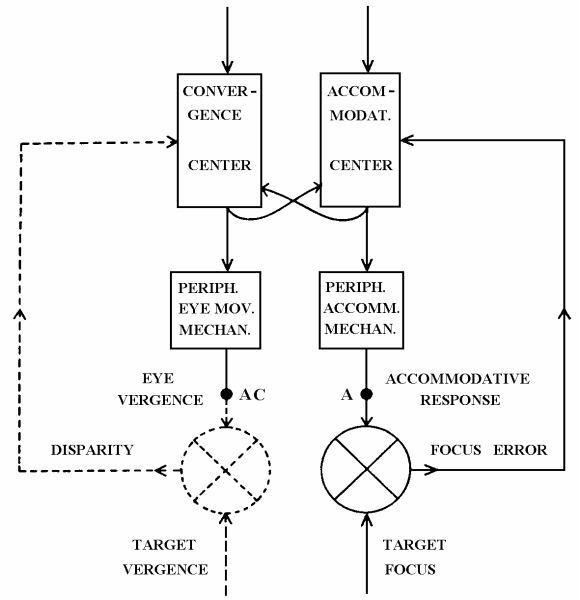

Figure 8.6. Westheimer's descriptive model of accommodation (right) and vergence (left) and their interactive connections. The peripheral accommodation mechanism represents the ciliary muscle, zonule, and lens, whereas the peripheral eye movement mechanism represents the extraocular muscles. Symbols: A = accommodative response; AC = accommodative convergence response when the vergence feedback loop is disabled (see dashed portion). Labels A and AC added for clarity. Adapted from Westheimer (1963), pg. 834, Fig. 4, with permission of American Medical Association.

experiments, he proposed central interactions between accommodative and vergence centers. Thus, if the convergence feedback loop is disabled, for example with monocular viewing, accommodation can still drive convergence via its central interactive connection (i.e., accommodative convergence). This provides a measure of the accommodative convergence (AC) to accommodation (A), or the AC/A ratio. Similarly, if the accommodative loop is disabled, for example with pinhole viewing, convergence can still drive accommodation via its central interactive connection (i.e., convergence accommodation). The details of these interactive processes, however, are the topics for Chapter 9 in this volume. In the present chapter, the models will concentrate primarily on the accommodation system.

8.3.2 Toates model

Toates (1972a) proposed a similar descriptive block diagram model of the accommodation system, but using a more conventional configuration (Fig. 8.7a). He incorporated elements for the depth-of-focus (DOF), neural controller, and ciliary muscle for driving the lens response. In addition, he proposed a more detailed descriptive model of the accommodation system (Fig. 8.7b; Toates 1972a,b).

Although he did not simulate the model, he reasoned that based on a general negative-feedback control system (Fig. 8.8a), there are two possibilities for control of accommodation. First, the system can operate with proportional control in the forward loop (Fig. 8.8b), so that the output is proportional to the error. That is,

$$\text{output} = \text{K} \bullet \text{error} \tag{8.1}$$

where K is the forward-loop gain. Toates derived equations in the feedback model for both the output and error as a function of input:

$$\text{output} = \frac{\text{K}}{1+\text{K}} \bullet \text{input} \tag{8.2}$$

$$\text{error} = \frac{1}{1+\text{K}} \bullet \text{input} \tag{8.3}$$

Substituting Eq. 8.3 into 8.2 gives Eq. 8.1, which provides a consistency check for these equations.

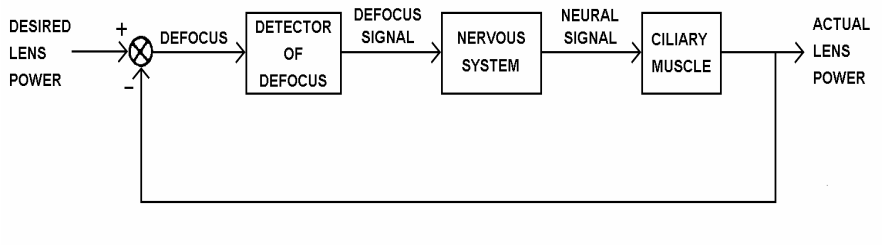

Fig. 8.7a. Descriptive model of the accommodation system. Reprinted from Toates (1972a), pg. 843, Fig. 2, with permission of Physiological Reviews.

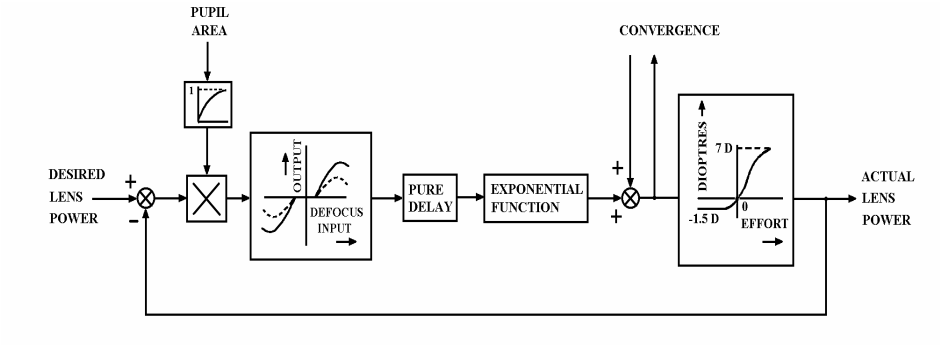

Fig. 8.7b. Toates' (1972a) detailed descriptive model of the accommodation system. The actual lens power is subtracted from the desired lens power to provide the accommodative error. The "detector of defocus" element shown in Fig. 8.7a is replaced here by a multiplicative element and a defocus input-output element. Thus, the accommodative error is multiplied by a value associated with pupil area to result in retinal defocus. The defocus is input to a functional relationship whose neural signal output is dependent on whether the illumination and/or visual acuity is high (solid) or low (dashed). Note that the output declines for large defocus values. The "nervous system" element in Fig. 8.7a is represented here by the delay and exponential function elements. The pure delay represents the amount of time the system takes to process the stimulus information. The exponential function is meant to produce an exponentially-shaped response to a step input. The arrows to and from "convergence" represent the interactive signals to and from the vergence system. Finally, the "ciliary muscle" output in Fig. 8.7a is replaced by a plant element with a negative limit at -1.5 D and a saturation limit at 7D. Adapted from Toates (1972a), pg. 847, Fig. 5, with permission of Physiological Reviews.

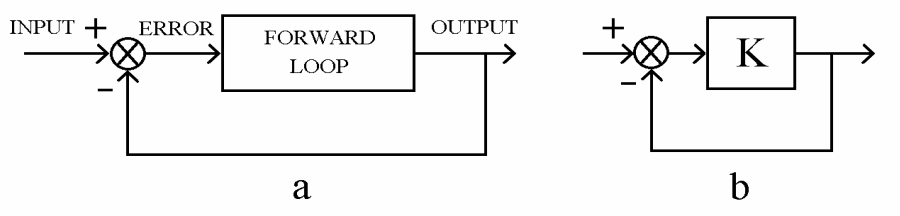

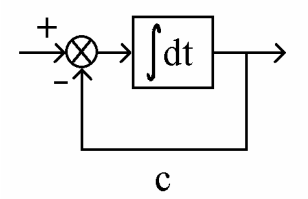

Fig. 8.8. Toates (a) general; (b) proportional; and (c) integral negative-feedback control systems. Reprinted from Toates (1972a), pg. 845, Fig. 3, with permission of Physiological Reviews.

The evidence for proportional control in the accommodation system can be seen in the lag of accommodative response in the linear region of the AS/R curve (Fig. 8.2), where the steady-state AR is approximately a fixed fraction of AS (see Eq. 8.2). If one were then to plot AR vs. AE, using the data from Fig. 8.2, it can be shown that AR is proportional to AE. Thus, the steady-state accommodative data are consistent with Eq. 8.1, which provides support for a proportional control system.

Second, the system can operate with integral control in the forward loop, so that the output is the integral of the error (see Fig. 8.8c, where the integrator in Laplace notation would be equal to 1/s):

$$\text{output} = \int_0^t \text{error} \bullet dt \qquad (8.4)$$

It can be seen in Eq. 8.4 that if the error is a non-zero constant, the output would be equal to the integral of that constant and would continue to grow. Conversely, the only way the output can remain at a constant value is for no additional integration to take place. This can only occur if the error is zero (i.e., AR is on the 1:1 line). Toates (1972) reasoned that since the steady-state AS/R function exhibits a non-zero residual AE (i.e., AR is either above or below the 1:1 line), there could not have been an integrator in the model. Thus, he concluded that an appropriate model for the accommodation system used proportional rather than integral control.

However, Toates did not consider that a purely proportional control system would give instantaneous rather than relatively slowly-changing responses, as seen in the experimental time traces (see Fig. 8.3a-c). Indeed, Krishnan and Stark (1975) indicated that computer simulation of Toates' proportional control model exhibited unstable rather than smooth responses to step stimuli. It turns out that there is a compromise solution between proportional and integral controller. A controller that produces both a slowly-changing response and a non-zero steady-state error would have the form:

$$\frac{K}{\tau s + 1} \tag{8.5}$$

which is a "leaky integrator" (see definition below) with controller gain K and time constant τ (Krishnan and Stark, 1975).

8.3.3 O'Neill model

O'Neill (1969) proposed an integral control model of accommodation (Fig. 8.9). Simulation step response shape was similar to experimental curves. However, as discussed above, a pure integral control model would not be able to simulate accurately the steady-state response.

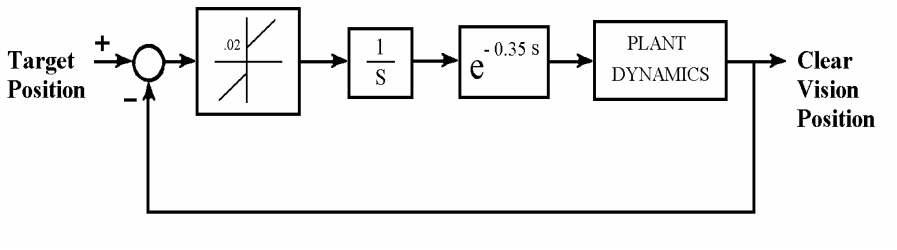

Fig. 8.9. Simplified O'Neill (1969) integral model of the accommodation system. The forward loop consisted of a threshold element, integrator, time delay, and plant dynamics. Target position and eye position are measured in diopters. Adapted from O'Neill (1969), pg. 654, Fig. 8, with permission of Elsevier Science.

8.3.4 Stark, Takahashi and Zames model

Stark, Takahashi and Zames (1965) derived an analytical model based on experimental frequency response data, which resulted in a rather complex transfer function (Fig. 8.10). However, to maintain stability in the simulation responses and to provide a good fit to the experimental data, they had to reduce the latency to 0.1 sec. This was much shorter than the 0.37 sec found experimentally (Campbell and Westheimer, 1960). Thus, while the model exhibited frequency response characteristics similar to experimental data, its latency was physiologically unrealistic.

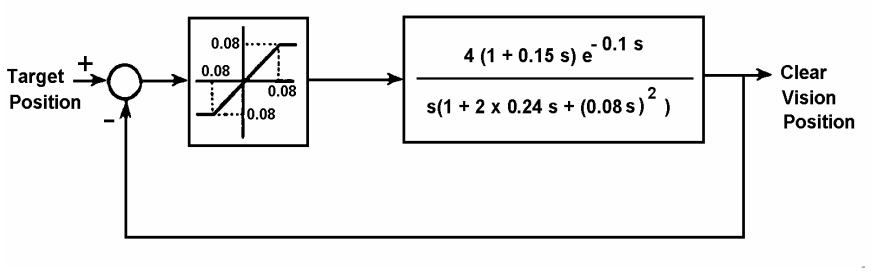

Fig. 8.10. Stark, Takahashi, and Zames (1965) feedback systems model of accommodation based on nonlinear servo-analysis of accommodation system frequency response. The Clear Vision Position is a measure of the refractive state of the lens; both the Target Position and Clear Vision Position are measured in diopters. The error signal is blur, and the effect of blur on the refractive state of the lens is modulated by the saturation nonlinearity. Note the latency was set at 0.1 sec rather than the experimental value of 0.37 sec to provide stable model simulation frequency responses. Reprinted from Krishnan and Stark (1975), pg. 78, Fig. 6, with permission of Elsevier Science.

8.3.5 Brodkey and Stark model

Brodkey and Stark (1967) also based their model on the above experimental frequency response data (see Sub-Section 8.3.4; Fig. 8.11) A derivative element, a static nonlinear element (i.e., a piecewise linear element), and a dynamic element with latency of 0.3 sec were introduced into the forward loop. Simulation results showed, however, that the phase predicted by this model lead the experimental phase-lag by 90 deg at low frequencies and lagged the experimental phase-lag by 90 deg at high frequencies. Hence, the dynamics of the model were problematic.

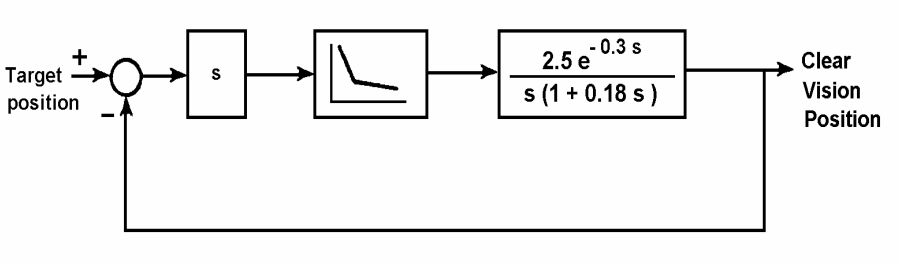

Fig. 8.11. Brodkey and Stark (1967) model of the accommodation system. This model is also based on frequency response data. Reprinted from Krishnan and Stark (1975), pg. 130, Fig. 24, with permission of Elsevier Science.

8.3.6 Krishnan and Stark model

Krishnan and Stark (1975) continued with the proportional and integral controller ideas and developed a model containing a "leaky" integrator along with other nonlinear elements (Fig. 8.12). Although the model exhibited simulation step responses with larger amplitude oscillations than the experimental data, it was able to account reasonably well for the decay of accommodation towards the tonic or empty-field position with a time constant of 6 sec.

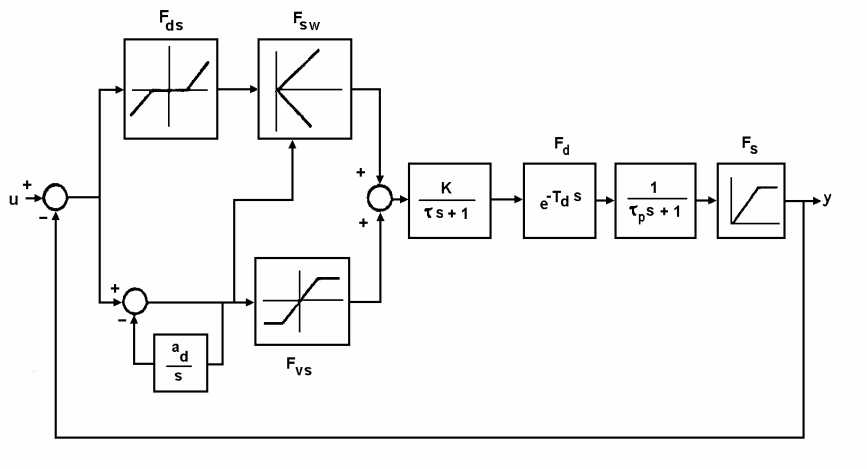

Fig. 8.12. Krishnan and Stark (1975) leaky-integrator model of the accommodation system. Symbols represent: u , target position; $a_d = 10$; $\tau = 10$ sec; $k = 4\tau$; $\tau_d = 0.38$ sec; $\tau_p = 0.4$ sec; F_{ds} , dead zone nonlinear element; F_{sw}, nonlinear switching element; F_{vs} , saturarion nonlinearity; y, clear vision position. Reprinted from Krishnan and Stark (1975), pg. 245, Fig. 8, with permission of Elsevier Science.

The numerous elements in the model are briefly describe as follows:

F_{ds} (deadspace operator). This represents the depth-of-focus, which allows for small neurosensory-based system errors to be tolerated without the perception of blur. If such neural tolerance were not permitted, we would be forced to have a perfect motor response at all times for clarity of vision, which is obviously an unrealistic expectation. Only if the input error exceeds this threshold level does it proceed to drive the system. The depth-of-focus is a function of pupil diameter, ranging from ± 0.15 D for an 8 mm diameter pupil to ± 0.85 D for a 1 mm diameter pupil (Campbell, 1957).

Nonlinear switching element (F_{sw}). Because blur is an even-error signal (i.e. , it lacks directional information), this element uses the sign information from the derivative operator to determine its direction. It generates a signal that is directionally correct and proportional to the magnitude of blur.

Derivative controller ($\frac{s}{s + a_d}$, derived from feedback loop containing $\frac{a_d}{s}$ in the feedback path). This parallel pseudo-derivative controller is a velocity operator. It generates the derivative of the error signal (i.e., the instantaneous velocity) for use by the control process. Such a controller improves the transient stability as well as the speed of the response.

Nonlinear saturation element (F_{vs}). This element is a velocity-sensitive component that prevents the response velocity from exceeding a certain limit. This, too, facilitates dynamic response stability and limits the amplitude of oscillations of the accommodative response.

"Leaky" integrator $\left(\frac{\tau}{\tau s + 1}\right)$**.** The "leaky" integrator is a "charge/discharge" element. It represents a central neurological integrating circuit that is rapidly activated ("charged" like an electronic capacitor) by the visual input and stores this information, thus providing for the initial steady-state maintenance of the response in the dark without visual information related to the target. Moreover, this circuit decays ("discharges") exponentially according to the value of its time constant, with the accommodative response shifting to the tonic accommodative bias level in 10 to 15 sec. In the model, the leaky integrator term is multiplied by 4, and thus the numerator in Fig. 8.12 is designated by K (= 4τ; where τ = 10 sec).

Time delay (F_d). This represents the combined neural and biomechanical transmission time delays, or latency.

Ciliary muscle/lens dynamics $\left(\frac{1}{\tau_p s + 1}\right)$. This represents the biomechanical response characteristics of the ciliary muscle/zonules/lens capsule complex, or "plant".

Saturation element (F_S). The saturation element limits the accommodative response imposed by the lens elasticity. In effect, it represents the maximum amplitude of accommodation (Hung, 1998; Ciuffreda, 1991, 1998).

8.3.7 Sun and Stark model

Sun and Stark (1990) followed up on Krishnan and Stark's (1975) nonlinear switching element concept and introduced a switching control model of accommodation (Fig. 8.13). The even-error nature of the blur signal is represented by a full-wave rectifying element. Thus, unlike previous models, the direction sense is assumed to be lost following the first element. Clearly, in a negative feedback control system, if the error signal is rectified, the system would rapidly go into instability oscillations. To prevent such a condition, they introduced a switching control technique. A switch-sensing element inserted after the rectifier block has three threshold levels, ON (0.7 D), OFF (slightly below 0.7 D), and "very large" (~4D, Neveu and Stark, 1995). If the absolute value of the error is either above ON or below "very large", thus representing the normal blur levels, the switch is closed, and a normal closed-loop response occurs. However, if the blur magnitude is either below OFF or above "very large", thereby representing either below blur threshold or very large blur conditions, respectively, the switch is opened, and the response decays towards the default tonic accommodative level.

The next element is a lag element with gain K=30 and time constant τ_1 = 2.5 sec. This is followed by a lead-lag, or a leaky integrator, with a time constant τ_2 = 30 sec. The output of this block is added with a white (i.e., broad-band) noise source (bandwidth = 0.3 sec^{-1}) having an average value of $\bar{n}$ = 0.5 D. The last block is the plant, which represents the zonular-lens complex. It contains a pure time delay of τ_0 = 0.1 sec. This latency is much less than that found experimentally, and presents the same problem in realistically simulating the accommodation system as the Stark et al (1965) model.

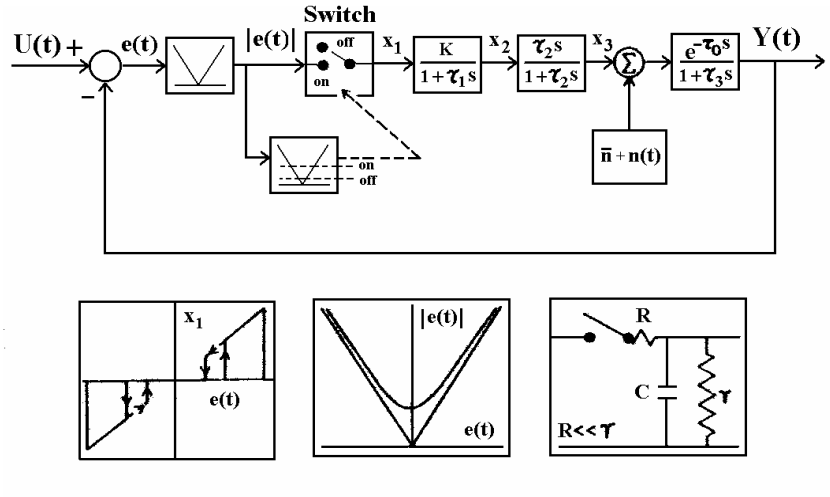

Fig. 8.13. Sun and Stark (1990) switching-control model of the accommodation system. Symbols represent: U= target position; Y = clear vision position, e = error between stimulus and response, or blur. Blur magnitude is input to a full-wave rectifier, resulting in even-error blur magnitude. The internal loop performs the switching function. Blur magnitude above ON threshold (0.7 D) closes the switch, resulting in normal closed-loop response; whereas blur magnitude that is either below OFF (representing the blur detection threshold; equal to "slightly less than 0.7 D") or is very large (with threshold set at ~ 4D) (Neveau and Stark, 1995), representing very large blur which also disables the accommodative response) opens the switch, resulting in an open-loop decay response. Noise n is added to the forward loop to mimic experimentally-observed high frequency accommodative oscillations. For blur magnitude outside this range, the switch is opened, and the response shifts towards the tonic level. Model parameter values: K=30; τ_0 = 0.1 sec; τ_1 = 2.5 sec; τ_2 = 30 sec; τn , the noise bandwidth = 0.3 (1/sec); $\bar{n}$ =0.5 D. Details of the switching mechanism in the inner loop are shown in the lower three panels. Lower left panel represents an imposed hysteresis relationship between X_1 and e(t) to reduce chattering (e.g., erratic rapid response changes) during switching. For positive e(t), switch ON follows the upward path, whereas switch OFF follows the downward path. Also, only |e(t)| is actually input into the switching operator. Lower middle panel represents the threshold based on geometrical and physical optics. Lower right panel represents equivalent electronic circuit diagram for the switch action showing an effective RC time constant during the switching operation. Reprinted from Sun and Stark (1990), pg. 76, Fig. 3, with permission of © IEEE.

Model simulation responses to increasing ramp stimuli were similar to experimental time traces. However, a closer analysis of the model indicated that the structure of the switch control sensor limits its responses. Due to the full-wave rectifying function, the system would not be able to respond to a decreasing stimulus such as a negative small amplitude step or ramp. This is because a negative error resulting from a decrease in accommodative stimulus would become a positive error following the rectifier function; and, if the amplitude is above ON, this would drive the response in the positive rather than negative direction. On the other hand, the model would appear to respond appropriately to a negative stimulus if its magnitude is above the "large" level. For example, a large downward step following a ramp, such as that seen in the simulations, causes the blur magnitude to be beyond this range, thus opening the switch, and the response will decay towards its tonic level. Hence, the large downward step movement seen following the ramp would not be a normal step response, but rather an open-loop decay movement.

8.3.8 Neveu and Stark model

The Neveu and Stark (Neveu and Stark, 1995; Stark et al, 2000) model is based on the Sun and Stark (1990) model, but with the addition of a schematic accommodation pathway (Fig. 8.14). Schematic accommodation represents the awareness of nearness of the target, or proximal accommodation, as well as other components such as voluntary accommodation and gaze/attention shifts. In addition, to overcome the inability to track negatively-directed accommodative stimuli (as discussed above for the Sun and Stark model), they used an odd- rather than even-error function for the "optics" component in the model (even though the symbol shown in Fig. 8.14 is for an even-error function). They simulated model responses to increasing and decreasing dioptric stimuli (in 1 D increments). For increasing stimuli (from 0 to 10 D), the simulated accommodative responses followed the target up to their pre-set presbyopic limit of 6 D. At that point, even as the stimulus steps continued to increase, the response decayed due to the presence of non-compensable retinal defocus and the resultant progressively reduced contrast gradient. However, when this was reversed, wherein the stimulus-decrease started from 10 D, the response remained at 1 D for stimuli above 5 D; but when the stimulus was $\leq$ 5 D, the response followed the stimulus (Fig. 8.15, left column figures). This directional difference in response based on its immediate past history is called hysteresis. Based on these simulation results, Neveu and Stark concluded that the behavior of the accommodation system depended both on the stimulus attributes and their immediate past history.

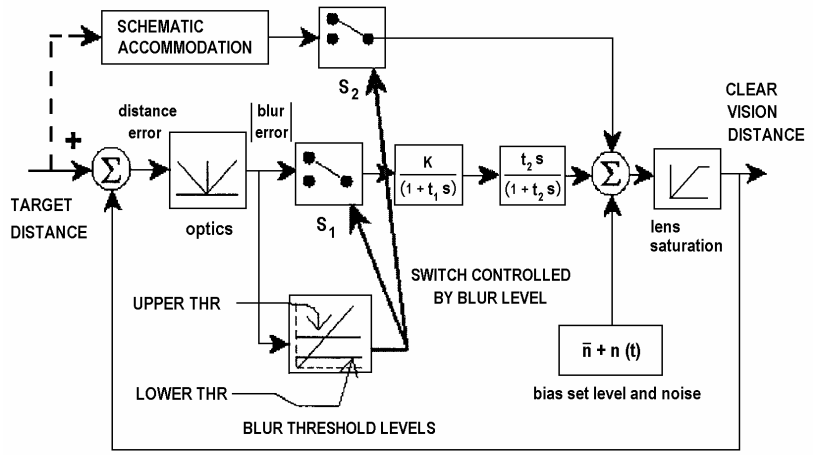

Fig. 8.14. Neveu and Stark (1995) blur switching control model of the accommodation system. Distance error, or blur, passes a rectifier to result in even-error blur magnitude. Mode 1: If blur magnitude is between the upper and lower thresholds (S1 closed) and schematic accommodation is absent (S2 open), normal feedback drives the accommodative response. Mode 2: If blur magnitude is outside of this region (S1 open) and schematic accommodation is absent (S2 open), the response drifts towards the tonic level. Mode 3: With voluntary effort for large accommodative error (i.e., blur error above upper threshold; S1 opened), schematic accommodation is activated (S2 closed) to drive the accommodative response. Reprinted from Neveau and Stark (1995), pg. 210, Fig. 6, with permission of Elsevier Science.

Analysis of this model indicates that there are two separate and distinct modes of action. For blur error magnitude between the upper and lower thresholds (S1 closed), the normal closed-loop response ensues, but without schematic accommodation (S2 open). On the other hand, for large blur error magnitude, voluntary or schematic accommodation (Neveu and Stark, 1995) is activated (S2 closed) to drive the response, but without normal closed-loop blur visual feedback (S1 open). This is consistent with the notion put forth by earlier investigators regarding the contribution from voluntary accommodation when blur error magnitude is very large (Fincham, 1951; Provine and Enoch, 1975; Ciuffreda and Kruger, 1988).

Simulation responses to decreasing step stimuli demonstrate the dichotomy between these two modes of action (Fig. 8.15). When only the closed-loop response is active (S1 closed; Fig. 8.15 left column figures), the range of responses is relatively small, but the error is also small. On the other hand, when only schematic accommodation is activated (S2 closed;

Fig. 8.15 right column figures), the range of responses is larger, but the error is also larger. These results are consistent with expected differences between normal closed-loop and voluntary accommodation (Fincham, 1951; Provine and Enoch, 1975; Ciuffreda and Kruger, 1988). However, examination of the simulated step responses reveal that they exhibit overshoots (Fig. 8.15), which are not seen in normal experimental step responses (see Fig. 8.3b; Campbell and Westheimer, 1959).

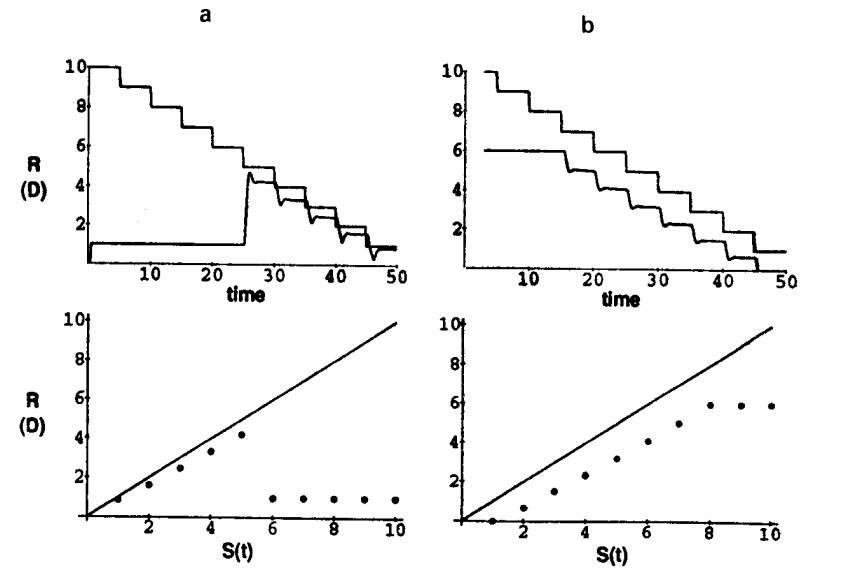

Fig. 8.15. Neveau and Stark (1995) model push-down simulation (10 to 0 D in 1 D increments). Top figure is simulation time course, and bottom figure is AS/R function. (a) Without schematic accommodation. Note an initial zero response until the stimulus is less than 5 D, at which point tracking begins and is fairly accurate. (b) With schematic accommodation. Note an initial 6 D until the stimulus is less than 6 D, at which point tracking begins, but the error is fairly large. In both (a) and (b), note the overshoot in the individual step responses, which is not seen experimentally. Reprinted from Neveu and Stark, (1995), 214, Fig. 10, with permission of Elsevier Science.

8.4 PRESENT MODELS OF ACCOMMODATION

8.4.1 Static models

There have been a few analysis and modeling attempts aimed at quantitatively generating an appropriate AS/R function (Fig. 8.2). They included a single index approach, incorporation of a sensory gain element in a feedback model, full feedback loop simulation, and finally, application of the model to amblyopia.

Chauhan and Charman (1995) proposed a single figure index for the steady-state accommodative stimulus/response profile (Fig. 8.2). It is based on the mean of the magnitude of the integrated accommodative error over the linear portion of the AR/S curve (i.e., the area bounded by the 1:1 line on top and AR below, over a range of AS values). They suggested that this index would provide a basis for comparison among different investigations. However, differences in the depth-of-focus (where one of its two boundaries is parallel to and just below the 1:1 line) among individuals would influence the effective area measures. Also, since this model can only be used over the linear range, it is somewhat limited as a general model of accommodation.

Hung (1997, 1998) proposed to simulate the static, or steady-state, AS/R function by driving a dynamic model with a series of step stimuli of various amplitudes and record the steady-state values. A descriptive block diagram of the model is shown in Fig. 8.16a. It is similar to Toates' (1972a) descriptive model (Fig. 8.7a), except that it also includes a latency and tonic element. A more detailed version of the model is shown in Fig. 8.16b. The deadspace element (with "breakpoints" at ±DSP) represents the depth-of-focus (DOF). The accommodative controller gain (ACG) represents the central neurological control of accommodation. The tonic term, ABIAS, represents the state of accommodation when the system is rendered open-loop, and it has been called "dark focus" and "night myopia" in the past (Westheimer, 1957; Liebowitz and Owens, 1978; Morgan, 1944; Hung and Semmlow, 1980), but is more appropriately called "tonic accommodation" (TA) since it is obtained under a wide range of conditions including darkness, empty field, and pinhole-viewing (Phillips, 1974). Gilmartin and Hogan (1985) found that parasympathetic innervation to the ciliary muscle plays a significant role in determining the TA position, and that the variation in TA among individuals is a consequence of parasympathetic rather than sympathetic ciliary muscle tone. The saturation element (Sat) of the plant limits the amplitude of the lens response. This decline in lens responsiveness with age represents the clinical condition of presbyopia (Mordi and Ciuffreda, 1998). Finally, a SIMILINK block diagram of the

model was constructed (Fig. 8.16c). A unique feature of this program is the stimulus, which is composed of a staircase series of steps of increasing amplitude. The program performs the multi-step simulations automatically. It records one steady-state value at the end of each step response, and continues until the last step stimulus is completed. After the simulation is completed, the data are plotted as AS/R curves. This is repeated for different model parameter values.

Fig. 8.16. (See next page). Hung's (1998) accommodation system models. (a) Descriptive model. The difference between target distance and focus distance provides the retinal-image defocus whose sensory output, or blur, is processed by the accommodative controller following a time delay. The controller output is summed with the tonic signal to drive the accommodative plant, or lens. The feedback loop reduces the blur to a minimum to provide clear focus of the target image on the retina. (b) Parametric model. The difference between accommodative stimulus and response, AS − AR, provides the accommodative error (AE). The AE is input to the deadspace operator, which represents the depth-of-focus, with threshold limits or breakpoints at ± DSP. The output of the deadspace operator, AE1, drives the accommodative controller consisting of gain ACG and a unity-gain dynamic transfer function, following a time delay. The output of the controller is summed with the tonic level, ABIAS, to drive the accommodative plant. The plant is represented by a saturation element, Sat, whose saturation point or level decreases with age. (The dynamic elements are shown as dashed blocks). (c) MATLAB4.1/SIMULINK1.3 simulation model. This is the model used for the simulations. The difference between the stimulus (which has a gapped-staircase pattern with period = 10 sec and dioptric increment = 0.1 D) and the system response is input to the deadspace operator (breakpoints at ± DSP). The deadspace operator output is input to the controller with gain ACG and transfer function 1/(s+1) following a time delay. The controller output is summed with the tonic level, ABIAS, to drive the plant, which is represented by a soft saturation element. The steady-state levels are obtained by sampling once every 10 sec to give the static stimulus and response functions, x and y, respectively. The static data are then plotted for different parameter values. Reprinted from Hung (1998), pg. 336, Figs. 2A-C, with permission of © IEEE.

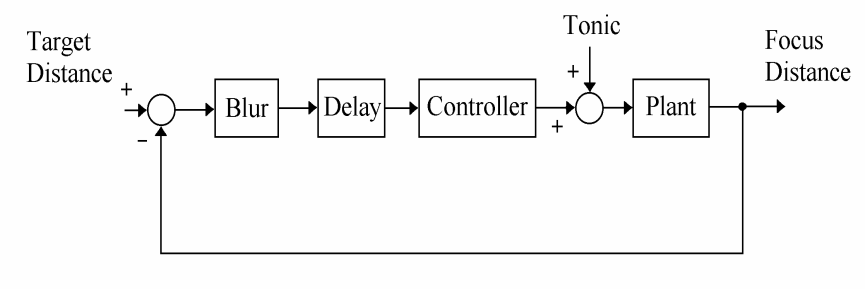
Target
Distance
+
−
Blur
Delay
Controller
Tonic
+
+
Plant
Focus
Distance

(a)

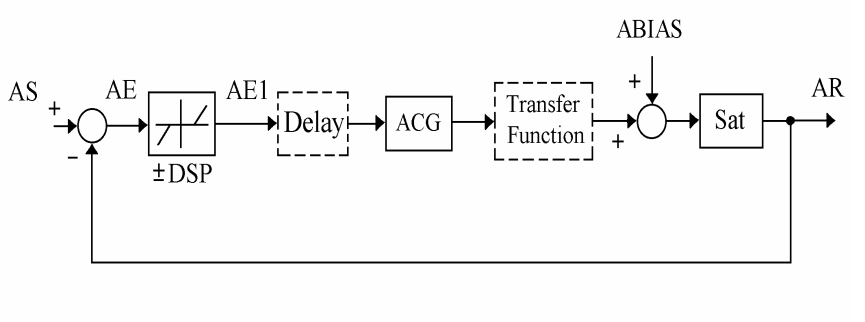
AS
+
−
AE
±DSP
AE1
Delay
ACG
Transfer
Function
ABIAS
+
+
Sat
AR

(b)

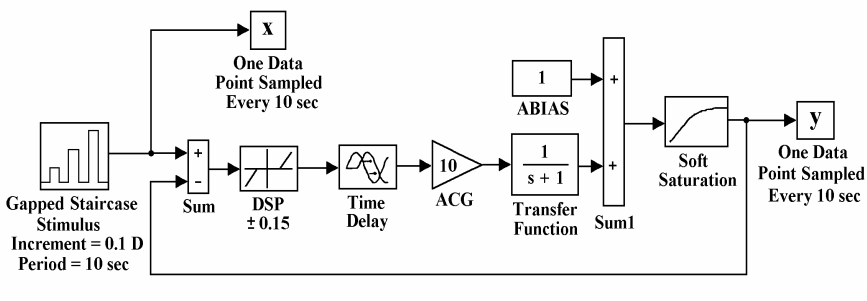
x
One Data
Point Sampled
Every 10 sec
Gapped Staircase
Stimulus
Increment = 0.1 D
Period = 10 sec
+
-
Sum
DSP
± 0.15
Time
Delay
10
ACG
1
ABIAS
1
s + 1
Transfer
Function
+
+
Sum1
Soft
Saturation
y
One Data
Point Sampled
Every 10 sec

(c)

Fig. 8.16

The simulated AS/R curve consisted of three regions demarcated by a deadspace region, which is the region bounded by two parallel lines (dashed) on either side and equidistant (= DSP) from the 1:1 line (e.g., see subplot with normal parameter values in Fig. 8.17c). For small AS levels, the AR is above the deadspace region, thus exhibiting the well-known "lead of accommodation". On the other hand, for large AS levels, the AR is below the deadspace region, thus exhibiting the well-known "lag of accommodation". Simulation results also show a transition region in which

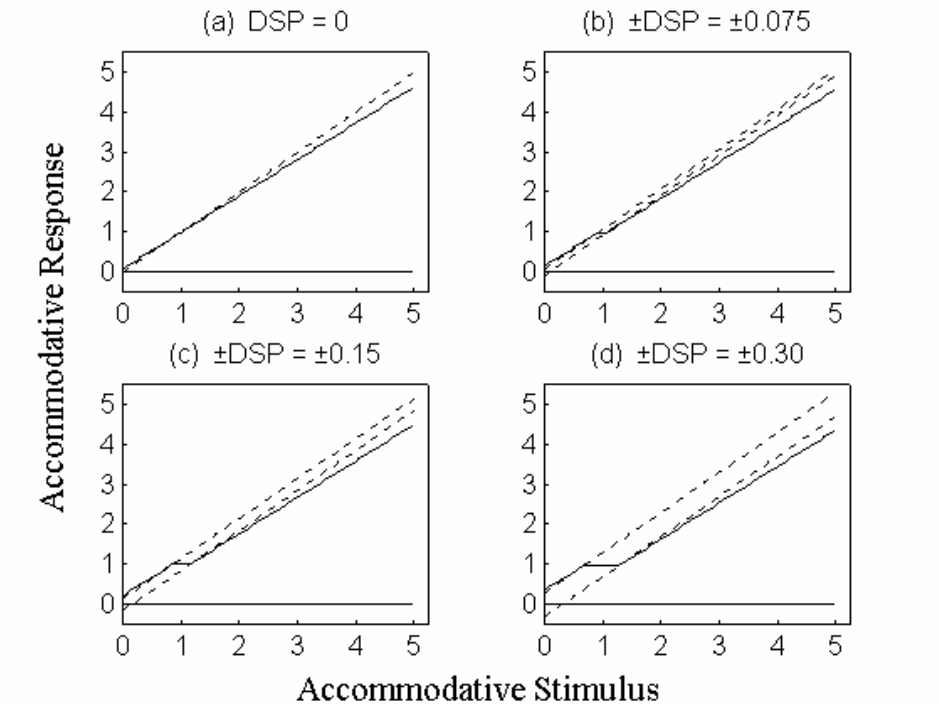

Fig. 8.17. Sensitivity analysis of the model AS/R relationship to variation in the parameter DSP (nominal values ±DSP = ±0.15 D, ACG = 10, ABIAS = 1.0 D, age ≤ 30 yrs.). For all four subplots, the dashed line respresents the limits of the deadspace (±DSP), and the solid lines represent the simulation results. The AS/R to the right of the deadspace line begins at the response level equal to ABIAS (Hung, 1998). The slope is equal to ACG/(1 + ACG). Similarly, the curve to the left of the deadspace lines begins at a response level equal to ABIAS and has the same slope. It can be seen in the four subplots that increasing DSP increases the horizontal width of the deadspaces. However, slope of the AS/R curve in the linear region remains the same. Reprinted from Hung (1998), pg. 338, Fig. 4A, with permission of © IEEE.

the response curve remains flat and equal to ABIAS, and this occurs entirely within the limits of the deadspace. The simulated AS/R curve (Fig. 8.17c) exhibits a shape similar to experimental results (see Fig. 8.2). At the crossover region, the experimental responses show more "rounded corners" than the model simulation curve. This can be explained, however, by the relatively wide spacing between stimulus values (e.g., 0, 1, and 2 D) that are typically taken for the AS/R curve. Smoothing of a curve through these relatively sparse experimental data points would obscure the underlying flat region, and result in the classical S-shaped AS/R curve. The relatively flat transition region can be more easily examined when the DOF is larger. Simulation results show that increasing ±DSP increases the DOF region about the 1:1 line (Figs. 8.17a-d), and produces a wider and flat transition region. Experimentally, this is observed in the AS/R curves for decreasing pupil size (Ripps et al., 1962) and increased target blur (Heath, 1956b).

The simulation results for varying ACG are shown in Fig. 8.18a. Increasing accommodative controller gain increases the slope of the AS/R curve. Note that the inflection of the curve occurs at AR level equal to ABIAS for all the different ACG curves. This is predicted from analysis of the model (Hung, 1998). Data for normal (+) and amblyopic (O) (an anomaly of vision in which there is a reduction in monocular visual acuity that is not correctable by refractive means and is not attributed to obvious structural or pathological ocular defects; Ciuffreda and Kenyon, 1983; Hung and Ciuffreda, 1983; Ciuffreda et al, 1991; Hung, 1998) eyes are presented. Since normal ACG (~ 10) is maintained by central neural control, the reduction in slope seen in the amblyopic eye indicates a central neural deficit of sensory origin. Indeed, values of ACG have been found to be a useful indicator of the amblyopic deficit (Ciuffreda et al, 1984, 1992).

The simulation results for varying ages are shown in Fig. 8.18b. With increasing age, the saturation level decreases, while maintaining the same normal AR and slope for values below the saturation level. This is consistent with the Hess-Gullstrand (Hess, 1904; Stark, 1987) theory of presbyopia, in which the lens and its surrounding capsule become less responsive with age, thus reducing the maximum level of accommodation. Representative experimental data for different age groups are also shown (Hung and Semmlow, 1980; Ripps et al, 1962; and Ciuffreda et al, 1997, 2000; Mordi and Ciuffreda, 1998). Age-related changes in model parameter values have been experimentally determined (Tables 8.1 and 8.2).

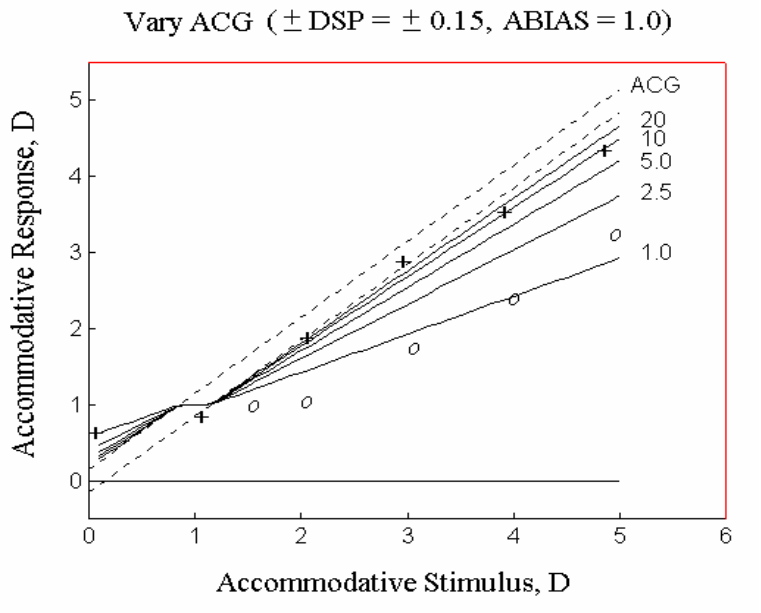
Vary ACG (± DSP = ± 0.15, ABIAS = 1.0)
Accommodative Response, D
Accommodative Stimulus, D
ACG
20
10
5.0
2.5
1.0
0
1
2
3
4
5
6

(a)

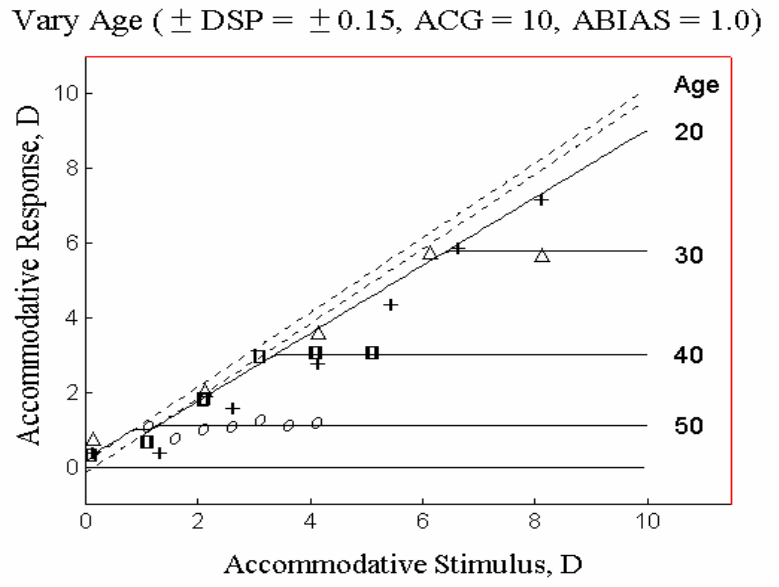
Vary Age (± DSP = ± 0.15, ACG = 10, ABIAS = 1.0)
Accommodative Response, D
Accommodative Stimulus, D
Age
20
30
40
50
0
2
4
6
8
10

(b)

Fig. 8.18

Fig. 8.18. (See previous page). Sensitivity analysis of AS/R function to variations in (a) ACG and (b) age. (a) Increasing ACG from 1.0 to 20 results in a progressive increase in slope, where the simulation slope is equal to ACG/(1 + ACG). The inflection of the curve at the level equal to ABIAS remains the same. Also plotted are experimental data for normal (+ symbol; corresponding to ACG ~ 10) and amblyopic (O symbol; corresponding to ACG ~ 1) subjects. The reduction of gain in the amblyopic eye indicates a central neural deficit. (b) Increasing age from 20 to 50 years results in a progressive decline in the saturation level, without a change in slope in the linear region. Also plotted are experimental data for subjects aged 20 (+ symbol), 32 (Δ symbol), 37 (Y symbol), and 49 (O symbol) years. The constant slope of the AS/R curve up to the saturation level for each of the groups supports the Hess-Gullstrand theory of presbyopia (Ciuffreda et al, 1997). Reprinted from Hung (1998), pg. 338, Figs. 4C-D, with permission of © IEEE.

Table 8.1. Oculomotor parameters and age. Reprinted from Ciuffreda et al (2000) with permission of Birkh←user Verlag.

Increase	Decrease	Constant
Subjective depth-of-focus	Accommodative amplitude	Objective depth-of-focus
Accommodative latency	Tonic accommodation	Open-loop gain
	Accomm. microfluctuations	Closed-loop gain
	Accommodative adaptation	Accommodative time const.
	CA/C ratio	Stimulus AC/A ratio
	Proximally-induced accomm.	Response AC/A ratio
		Peak vel./amp. relation
		Proximally-induced vergence
		Tonic vergence
		Vergence adaptation

Table 8.2. Rate of parameter change per year with increasing age. Reprinted from Ciuffreda et al (2000), pg. 197, Tables 1 and 2, with permission of Birkh←user Verlag.

Parameter	Annual rate of change
Subjective depth-of-focus	0.027 D
Accommodative latency	2.5 msec
Accommodative amplitude	0.34 D
Tonic accommodation	0.04 D
Accommodative microfluctuations	-
Accommodative adaptation	0.034 D
CA/C ratio	0.006 D/Δ
Proximally-induced accommodation	0.008 D

Jiang (2000) used the accommodative loop portion of the Hung and Semmlow (1980) model (Fig. 8.19a) to simulate the AS/R function. In the Hung and Semmlow model (1980), the depth-of-focus (DOF) was represented by a deadspace element with breakpoints at ±DSP, and the value for DSP was assumed for simplicity to be a constant. Jiang noted, however, that target luminance (Johnson, 1976) affected the pupil size, which in turn modified the depth-of-focus. Moreover, variation in target blur (Heath, 1956b), spatial frequency (Ciuffreda and Hokoda, 1983) and contrast (Ciuffreda and Rumpf, 1985) influenced the effective DOF, without changing the pupil size. To account for these influences, he introduced an accommodative sensory gain (ASG) element in front of the deadspace element (Fig. 8.19b). Thus, the accommodative error, AE, is multiplied by ASG, and the product is input to the deadspace element. The model was simulated by Hung (2001, unpublished) using a modified form of Fig 8.16c by inserting an ASG gain element between the summing junction and the deadspace operator. Simulations were performed for various values of ASG (0.2 to 1.6 in 0.2 increments) while holding the other parameters constant (±DSP = ±0.15, ACG = 10, and ABIAS = 1.0) (Fig. 8.20). The ASG value was limited to 1.6 because higher values resulted in instability oscillation.

The simulation results revealed that the ASG affects both the effective deadspace limits and the slope of the linear portion of the AS/R function. The effect on the deadspace limits is due to the multiplication of DSP and 1/ASG, so that the effective deadspace limits are ±AE/ASG. That is, the "effective" deadspace limits determine the actual boundaries of the deadspace region. Thus, for example, if ASG=0.2, and the nominal deadspace limits are equal to ±0.15 D, the effective deadspace limits become ±0.75 D. This means that to drive the accommodative controller, the accommodative error (AE) needs to be greater than +0.75 D or less than -0.75 D.

The increase in slope of the linear portion of the AS/R curve with increasing ASG (see Fig. 8.20) is predicted by the following equation (Jiang, 2000):

$$\text{slope} = \frac{\text{ASG} * \text{ACG}}{1 + \text{ASG} * \text{ACG}} \tag{8.6}$$

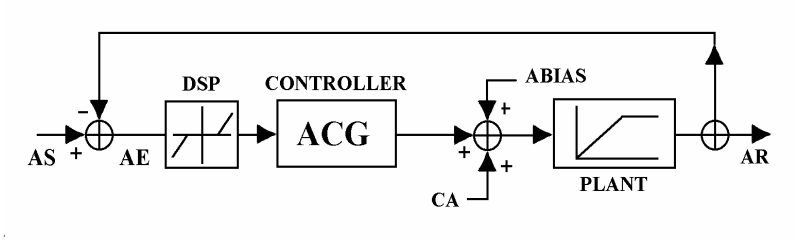

(a)

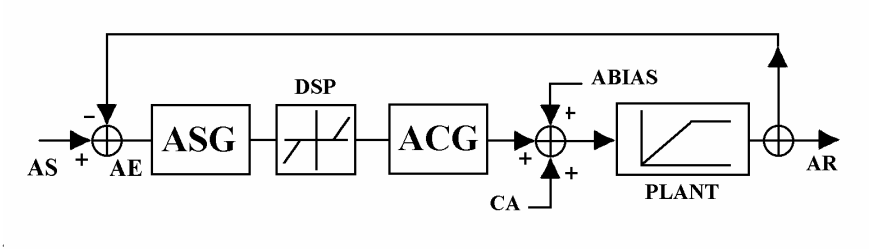

(b)

Fig. 8.19. (a) Accommodative loop of the Hung and Semmlow model (1980) showing deadspace operator DSP, accommodative controller gain ACG, tonic accommodation ABIAS, accommodative saturation element PLANT, and convergence accommodation crosslink input CA. (b) An accommodative sensory gain (ASG) element was placed in front of the deadspace element to account for the effect of reduced stimulus effectiveness (blurring; decreased spatial frequency, contrast, or luminance) on the effective DOF. Reprinted from Jiang (2000), pp. 236, 239, Figs. 1, 2, with permission of Birkh←user Verlag .

Table 8.3 lists the slope as a function of ASG. It can be seen that for ASG from 0.2 to 0.4, there is a substantial increase the slope, whereas for larger ASG values from 0.4 to 1.6, there is a progressive but relatively smaller increase in slope from 0.80 to 0.94.

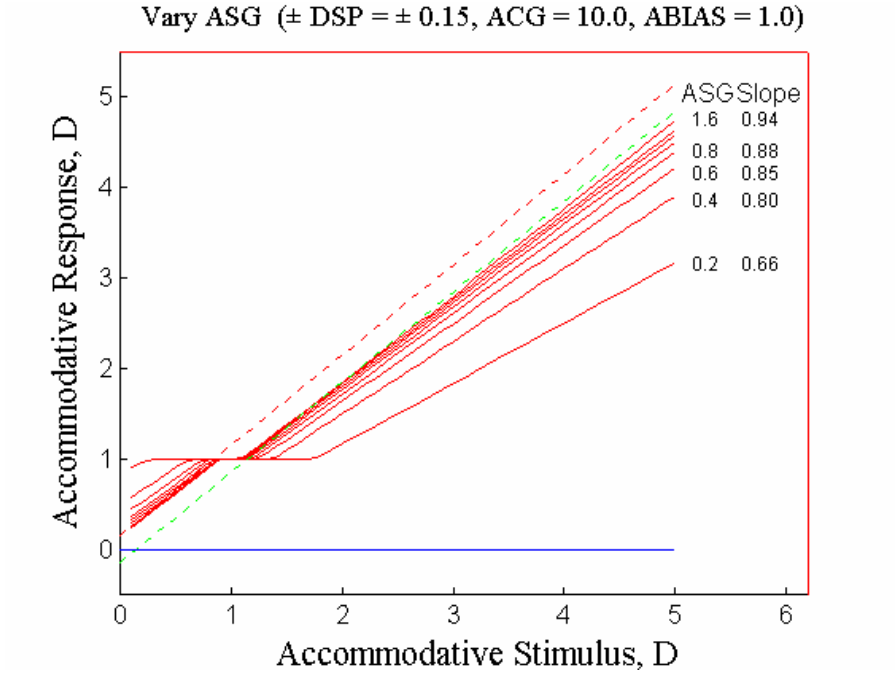

Fig. 8.20. Sensitivity of AS/R function to variations in ASG (0.2 to 1.6 in 0.2 increments) while other parameters of Jiang's (2000) model were held constant. Dashed lines represents the limits of the nominal deadspace region (DSP = ±0.15 D) about the 1:1 line. Note the increase in effective deadspace with decreasing ASG. Also, except for a substantial increase in slope for ASG between 0.2 to 0.4, the slope increases progressively but slightly as ASG is increased from 0.4 to 1.6 (see Table 8.3). From Hung, personal communication (2001).

Table 8.3 - Effect of ASG on slope of the linear portion of the AS/R curve

ASG	0.2	0.4	0.6	0.8	1.0	1.2	1.4	1.6
Slope	0.67	0.80	0.86	0.89	0.91	0.92	0.93	0.94

In addition to the above models, a conceptual model was developed by Ciuffreda et al (1991; Fig. 8.21) to examine the factors associated with the amblyopic accommodative deficit. It was based experimental findings in amblyopic eyes focusing on sine- and square-wave spatial stimuli (Ciuffreda et al., 1991). They showed an overall reduction in the accommodative response level in the amblyopic eye as compared with the fellow normal eye, but normal consensual responses in the amblyopic eye when driven by the fellow eye. This suggested that the site of the accommodative dysfunction was neither the motor controller nor the peripheral apparatus, but rather was in the sensory controller. Such a sensory deficit was presumed to be due to the early, prolonged abnormal visual experience. In terms of the model of steady-state accommodation (Hung, 1998), the accommodative defect was

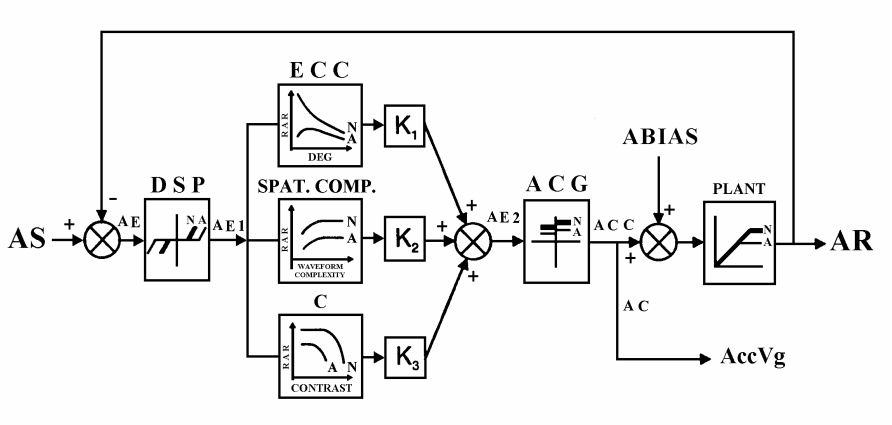

Fig. 8.21. Ciuffreda et al (1991) static model of the accommodation system, with inclusion of several of the sensory factors that account for much of the reduced accommodative responses found in amblyopic eyes. These include target retinal eccentricity (ECC), spatial composition (SPAT. COMP.), and contrast (C), with K_1, K_2, and K_3 being gain terms, and RAR being the relative accommodative response. Accommodative error (AE) is the difference between accommodative stimulus (AS) and accommodative response (AR). Deadspace (±DSP) reflects depth-of-focus of the eye. Output (AE1) from the deadspace operator goes into the accommodative controller, which exhibits nonlinear accommodative gain (ACG). Output (ACC) from the accommodative controller is summed at the summing junction (⊗) and also cross-linked to the vergence system (Acc Vg) by means of gain AC. Accommodative bias (ABIAS) or tonic accommodation under the "no stimulus" (i.e., open-loop accommodation and vergence) condition is also summed here. Output from the summing junction goes through a saturation element, which reflects plant saturation of the accommodation system. N and A are normal and amblyopic eyes, respectively. Reprinted from Ciuffreda et al (1991), pg. 299, Fig. 6.30, with permission of K. J. Ciuffreda, the copyright holder.

believed to be localized at the site of the accommodative controller gain (ACG in Fig. 8.16b), resulting in reduced response amplitude. In addition, such factors as abnormal fixational eye movements, defective contrast perception, and/or eccentric fixation may contribute to the reduced responsivity. Thus, in the conceptual model (Fig. 8.21), empirically-derived relationships for target-eccentricity, spatial composition, and contrast were placed in the forward loop to represent the various sensory factors that affect accommodative controller gain. This configuration is similar to the ASG element proposed more recently by Jiang (2000), except the sensory elements were placed after rather than before the deadspace operator. Such a model may be used clinically to simulate more accurately the various stimulus attributes that affect accommodative behavior in the amblyopic eye.

8.4.2 Dynamic models

8.4.2.1 Stability Analysis Using Root Locus

Campbell et al. (1959) analyzed the frequency spectrum of the steady-state accommodative response and found two spectral peaks, a larger peak at 2 Hz and a smaller peak at 0.5 Hz. The cause of these peaks had been unresolved for over two decades. Then, Hung et al. (1982) applied the root locus analysis technique (D'Azzo and Houpis, 1988) to a dynamic accommodation system (Fig. 8.22a) to determine whether these peaks were caused by system instability oscillations. This technique is a general method for quantifying the stability characteristics of a feedback system, with the forward loop as the controlling parameter. This method is well suited for evaluating the stability of the accommodation system and its dependence on ACG. However, the root locus method is only applicable to linear systems; hence, for this analysis a linear approximation is used in place of the nonlinear deadspace operator, or the DOF. As the accommodation system generally operates on one side of the DOF (the low-output side for normal near viewing, leading to the descriptive term "lag of accommodation") (Morgan, 1968), the deadspace operator can be appropriately replaced by a linear bias or "offset" term (Hung and Semmlow, 1980).

A root locus computer program developed by Krall and Fornaro (1967) was used to analyze the dynamic stability characteristics of the accommodation model (Hung et al, 1982). The unique feature of this root locus program is that it allows for a delay element (to simulate latency) in the feedback loop. The program plots the location of the closed-loop poles (equal to the roots of the denominator of the transfer function, so that when the system operates near the root value, the transfer function output rapidly

grows to an infinite value, hence the name pole) as a function of gain K for forward-loop transfer function of the form, $K\,e^{-\tau s}G(s)$, or overall closed-loop transfer function of the form

$$\frac{K\,e^{-\tau s}\;G(s)}{1+K\,e^{-\tau s}\;G(s)} \tag{8.7}$$

For the analysis of the accommodative system model, the following parameter values used were: controller time constant = 6 sec, plant time constant = 300 msec, and a total time delay = 350 msec. Thus,

$$Ke^{-\tau s}\;G(s)=\frac{Ke^{-\,0.35s}}{(1+6s)\,(1+0.3s)} \tag{8.8}$$

The root locus plot of the linearized accommodation system with forward-loop transfer function given by Eq. 8.8 is shown in Fig. 8.22b, where the horizontal and vertical axes are the σ and $j\omega$ axes, respectively. From this plot we note that the gain corresponding to the root locus at the $j\omega$ axis is equal to 21, which gives the maximum gain before instability oscillation occurs (i.e., poles in the right half of the s-plane, or to the right of the vertical jw axis, corresponding to a time domain function which grows rapidly, and would mean the system is unstable). The predicted frequency for instability oscillation of 0.45 Hz (or 2.8 rad/sec) is near the lower accommodative spectral peak at 0.5 Hz, but far below the higher peak at 2 Hz (Campbell et al, 1959). This indicates that loop instability is not a source of higher frequency accommodative oscillations. However, the smaller peak at 0.5 Hz may in fact correspond to the closed-loop oscillation frequency of 0.45 Hz indicated in the root locus plot. Moreover, Winn et al (1990) found a significant correlation between the arterial pulse frequency and the accommodative higher frequency peak. In addition, Gray et al (1993) analyzed the accommodative spectrum as a function of pupil diameter and found that whereas the low frequency peak varied with pupil diameter, the high frequency peak did not. Thus, they concluded that the lower accommodative frequency peak which was predicted by the root locus analysis is most likely associated with neurologically-controlled feedback instability oscillations, whereas the high frequency peak is an epiphenomenon due to the effect of arterial pulse on lens motion that is detected by the recording optometer.

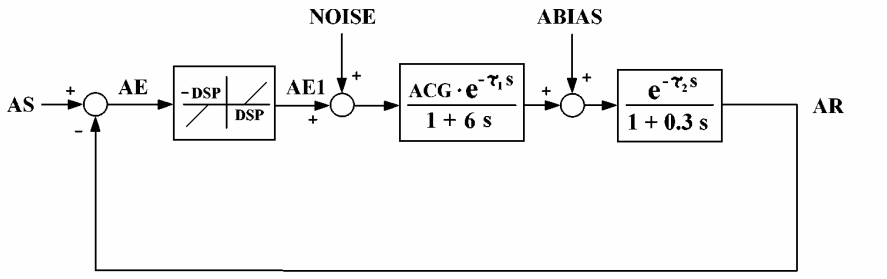

Fig. 8.22a. Accommodation model block diagram showing the difference between accommodative stimulus (AS) and accommodative response (AR) produces the accommodative error (AE). The output from the deadspace operator (± DSP = ± 0.30, which represents the depth of focus), AE1, is added to a 2 Hz noise signal and processed through the accommodative controller with gain ACG = 15, experimentally determined time constant of 6 sec, and delay τ_1 = 180 msec. The controller output is summed with tonic accommodation ABIAS = 0.5 D and processed through the plant representing the neuro-muscular apparatus with time constant 0.3 sec and time delay τ_2 = 170 msec to give the accommodative response. Reprinted from Hung et al. (1982), pg. 595, Fig. 2, with permission from © IEEE.

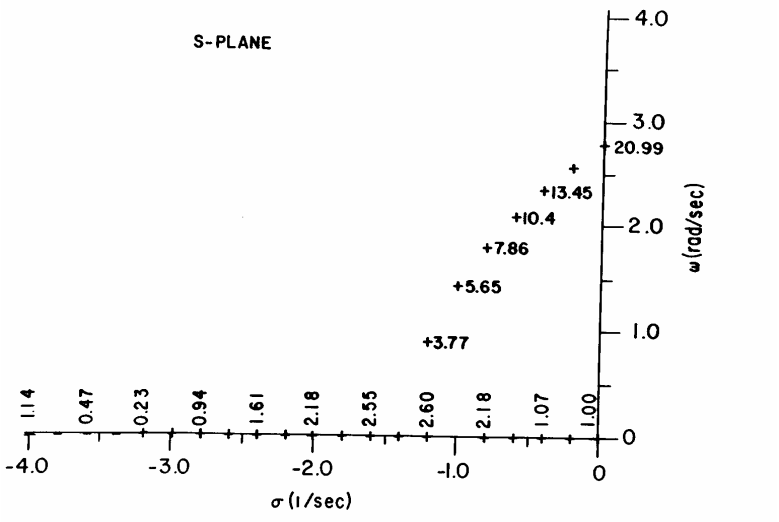

Fig. 8.22b. Root locus plot showing stability characteristics of the accommodation system. The accommodative controller gain, ACG, is used as a parameter in the root locus analysis. It can be shown that a closed-loop pole in the right half plane results in instability oscillations. This correspond to the ACG value of 21 with an instability frequency of ω = 2.8 rad/sec, or 0.45 Hz. Reprinted from Hung et al. (1982), pg. 597, Fig. 6, with permission from © IEEE.

8.4.2.1 Dual-Mode Dynamic Model of Accommodation

The difficulties encountered in previous continuous models of accommodation are not surprising (see Section 8.3). This is due to the inherent problem of having relatively slow dynamics (time constant = 250 msec) and a long time delay (350-400 msec) in a feedback loop. That is, the observed instantaneous accommodative output is actually a response to a controller signal (AE = AS - AR) that had occurred 370 msec earlier. If AE had changed sign (e.g., from positive AE, or lag of accommodation, to negative AE, or lead of accommodation) during the intervening delay interval, the accommodative output would be in the inappropriate direction. For dynamically changing accommodative stimuli, this could lead to repeatedly inappropriate responses, and in turn instability oscillations.

Switching control models were introduced to alleviate this problem. The idea was to switch the control mode based on a criterion level of a parameter, such as the blur magnitude. Although these models provided some reasonable simulations, they were not able to simulate a wide range of realistic and commonly encountered stimulus conditions. There were two main problems. First, they used incompletely defined criteria regimes, so that for example the model cannot respond to a negative ramp stimulus. Second, the model configuration did not provide appropriate dynamics, thereby resulting in unrealistic overshoots in the multiple-step responses for both closed-loop and voluntary or schematic accommodation.

To overcome all these difficulties, a dual-mode model of accommodation was developed (Fig. 8.23a-c; Hung and Ciuffreda, 1988; Khosroyani, 2000). It was based on the dual-mode model of vergence developed previously by Hung et al (1986) (see Chapter 9 in this volume). The underlying principle for the dual-mode model was evident in the experimental vergence responses to slow and fast ramp stimuli. For slow ramps, the responses followed the stimulus. However, for fast ramps, the responses consisted of a staircase series of step-like movements in which the end value of each step matched the ongoing ramp stimulus position. This indicated that there were two modes of operation. Thus, the key basis of this vergence model was that there were two mutually-exclusive modes of response: a fast, open-loop movement that corrected most of the error, followed by a slow, closed-loop movement that reduced the residual error to a minimum. Simulation of the dual-mode model showed accurate fit to a variety of experimental pulse, step, and ramp responses

Hung and Ciuffreda (1988) designed an experiment to determine whether dual-mode behavior for vergence as described above could also be present in the human accommodation system. Responses were recorded for accommodative ramp stimuli ranging from 0.5 to 5.0 D/sec. The results

showed that for ramp stimuli below 1.5 D/sec, the responses consisted of smooth tracking movements (see Fig. 8.4). On the other hand, for ramp stimuli above this value, the responses exhibited a staircase-like step behavior similar to that for the vergence system. Thus, the accommodative system was also shown to have dual-mode characteristics. However, Hung and Ciuffreda (1988) did not construct a dynamic model for accommodation.

Khosroyani (2000) constructed the first dual-mode dynamic model of the accommodation system using MATLAB/SIMULINK. Since both accommodation and vergence have been shown to exhibit dual-mode behavior (Hung et al, 1986; Hung and Ciuffreda, 1988), the same program used in the vergence dual-mode model (Hung et al, 1986; Hung, 1998) was used for these accommodative simulations, with appropriate parameter value changes. The overall block diagram of the model is shown in Fig. 8.23a. The first block is a deadspace operator which represents depth-of-focus, with limits equal to ±0.12 D. The controller consists of both fast and slow components. The fast component is derived from the sum of the visual feedback error signal and the neurological efference copy signal from the fast component output. The efference copy signal takes into account the effect of plant dynamics. This results in an open-loop signal that is nearly equal to the original stimulus amplitude. This open-loop drive is important for two reasons. First, it maintains stability in the presence of a relatively long latency (370ms); and second, it meets the requirement of an accurate initial step response. Such accuracy corresponds to very high gain in a feedback control system, which would have otherwise resulted in instability oscillations. The open-loop fast component movement accounts for most of the step response amplitude, with the reminder being taken up by the slow closed-loop component.

Fig. 8.23. (See next page). (a) Block diagram of the accommodation system used in MATLAB simulations. The difference between AS and AR, or AE, is input to a deadspace element, whose output is summed with the efference copy signal, resulting in a signal equal to the actual stimulus. This signal is used to drive the fast component. The output of the deadspace element also drives the slow component. The outputs of the slow and fast components are summed with the output of the sine-wave generator, which represents the microfluctuations, to drive the plant. The output of the plant provides the accommodative response. It is fed back and is subtracted from the accommodation stimulus to provide the error signal to the deadspace element. (b) The fast component operates in an open-loop manner, and it uses a sampler and has predictive capability for periodic stimuli. (c) The slow component operates under the closed-loop condition over a smaller range of accommodative error amplitudes and velocities. Overall, the fast and slow components operate over different stimulus regimes, so that when one is active, the other is disabled. This provides robustness in the model response (Hung, 1998; Khosroyani, 2000). Reprinted from Hung et al (1986), pg. 1023, Fig. 1, with permission of © IEEE.

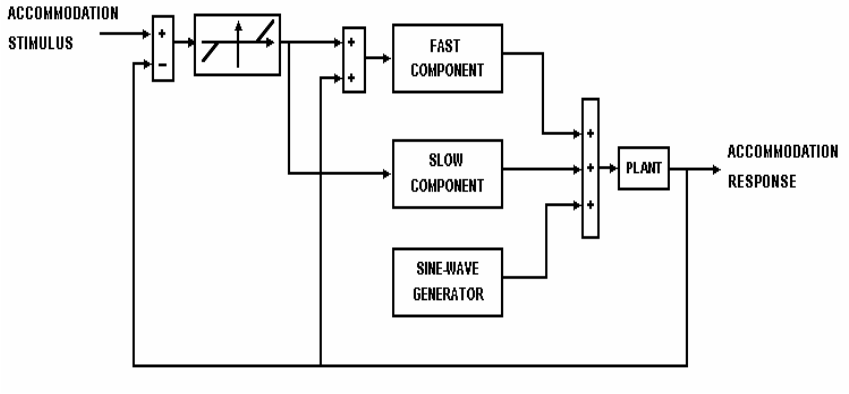

Fig. 8.23a. Overall block diagram of dual-mode accommodation model. See legend for details.

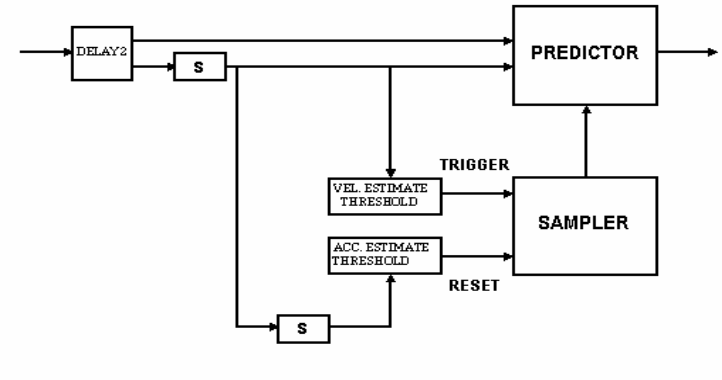

Fig. 8.23 b. Fast component.

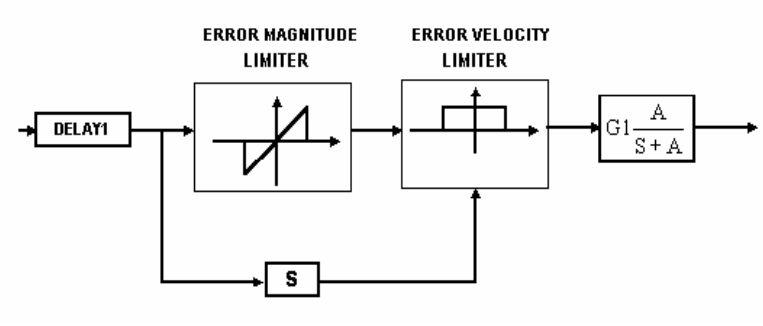

Fig. 8.23c. Slow component.

The block diagram for the fast component is shown in Fig. 8.23b. It receives a signal that represents the perceived target change. This is delayed by element 'DELAY2', which represents the effective delay throughout the fast component. The sampler and predictor act in conjunction to provide the sampling and predictive capabilities seen in the experimental ramp and sinusoidal responses. The sampler has a sensory threshold to account for the range of stimuli that elicit experimental sampling behavior. The sampler is triggered by a change in velocity of the perceived target above a given threshold. However, the sampler can be reset by a sudden change in target velocity, such as in a pulse stimulus. If the target velocity drops below a certain value, as in a step stimulus, the sampler is stopped. The sampler provides the timing control for the predictor. The predictor is a calculating unit that uses the target position and velocity information to estimate the future position of the target. The predictor estimates within the response latency where the target will be after a sampling interval, and then generates a step signal to correspond to the predicted new target position. For example, for a ramp stimulus, the predictor uses the target position and velocity information to estimate where the target position will be after a sampling interval and generates a characteristic step response which matches the target at the end of the sampling interval. If the ramp target continues, the predictor must recalculate after each sampling interval, so that the resulting staircase-like step response will again match the ramp stimulus. For step and ramp-step stimuli, which quickly reach and remain at the amplitude limit, the predictor determines the final value, and then generates a step signal to drive the response directly to the final position. For signals that regularly alternate, as in sinusoidal stimuli, the predictor serves another function. It reduces the time required for estimating the target position by reducing DELAY2, and hence decreases the phase lag between the accommodation stimulus and response. Thus, it represents the effect of anticipation of target motion.

The block diagram for the slow component is shown in Fig 8.23c. The slow component is driven by accommodation error, delayed by 370ms, and it has magnitude and velocity limiters to reflect the range of operation of the slow process. Its dynamics are modeled by a first-order lag element. The slow component acts over small amplitude and velocity ranges, and it uses negative feedback to provide the error signal for the controller. The fast and slow components operate under separate stimulus regimes, so that when one is active, the other one is disabled. This provide robustness in the accommodative response.

The other block in the overall model (Fig. 8.23a) is a sine-wave generator with 0.2D amplitude and 2 Hz frequency, which represents the high frequency microfluctuations as a plant noise (Campbell, 1959; Gray et al, 1993). This has been shown, however, to be derived from the cardiac pulse

signal that is picked as an artifact of the accommodation recording process (Winn et al, 1990). The outputs of the fast and slow components, and the sine wave generator, are summed and fed to the plant, which represents the dynamics of zonule, ciliary muscle, lens capsule, and lens The plant has a time constant of 0.3 sec based on ciliary muscle stimulation in the monkey (Thompson, 1975).

The simulation results are shown in Fig. 8.24a-c for: (a) pulse and square-wave; (b) ramp; and (c) sinusoidal stimuli. They are in reasonably good agreement with experimental results. The pulse response follows the on- and off-portions of the stimulus. (Fig. 8.24a). The ramp responses exhibit a transition from smooth tracking for slow ramp stimuli to steps and multiple-steps for faster ramp stimuli (Fig. 8.24b). Sinusoidal responses show a transition from smooth tracking by the slow component (stimulus frequencies at 0.05 and 0.1 Hz) to combined fast and slow component movements for higher frequency stimuli. (Fig. 8.24c). For the periodic stimuli (Figs. 8.24a and c), a reduction in latency (to represent prediction) is evident after a few cycles in many of the responses. Thus, the dual-mode model of accommodation is able to simulate reasonably accurately a wide variety of stimuli.

Fig. 8.24. (See next two pages). Dual-model accommodation model responses to: (a) pulse (top trace, 0.32 sec stimulus duration) and square-wave stimulation (frequency, in Hz, is shown at right of traces) of 2D amplitude; (b) ramp stimulation (velocity, in D/sec, is shown at right of traces) with maximum amplitude of 2D; and (c) sine-wave stimulation (frequency, in Hz, is shown at right of traces) for +/-2D peak-to-peak amplitude (Khosroyani, 2000). Dashed lines represent the stimulus, and continuous lines represent the response. Horizontal lines represent zero level of accommodation. For graphs (a)-(c), the ordinate is designated in diopters (D).

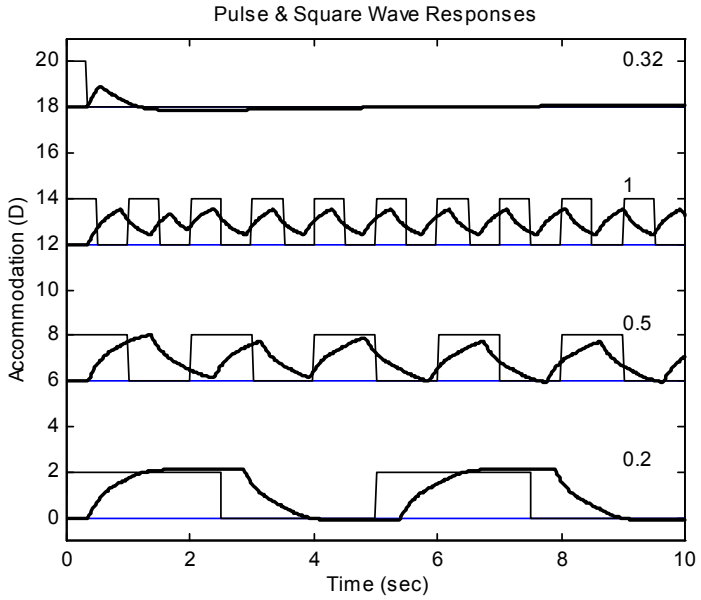

Fig. 8.24a.

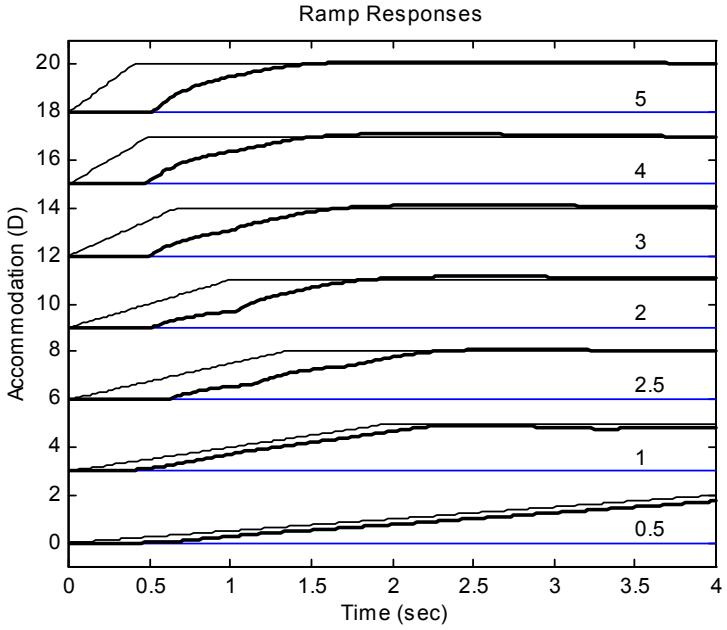

Time, sec

Fig. 8.24b.

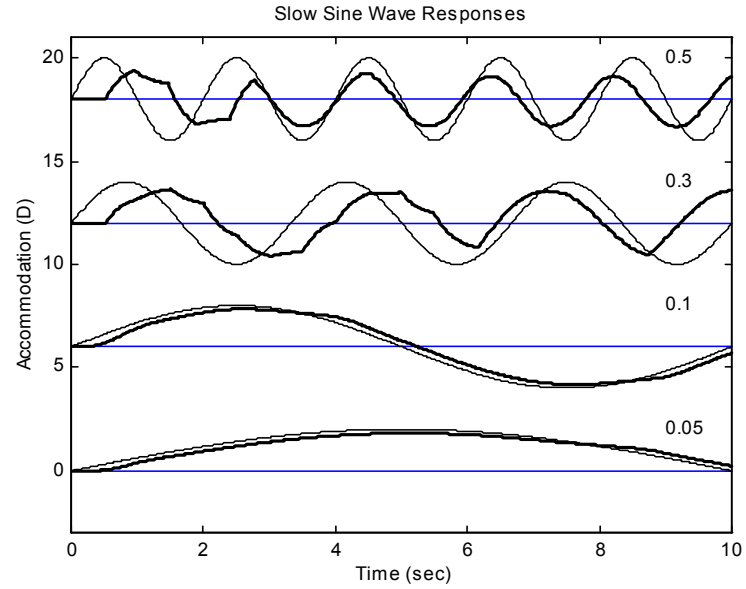

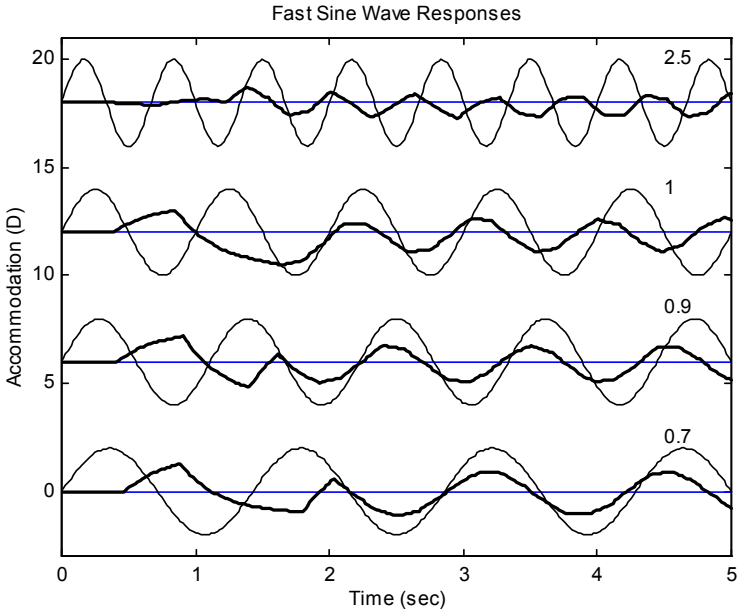

Time, sec

Fig. 8.24c.

In addition to the above dynamic models, Hung and Ciuffreda (Hung et al, 1996; Ciuffreda et al, 2000) developed a descriptive comprehensive model of accommodation and vergence that summarized the dual interactive nature of these systems (Fig. 8.25a; Hung and Semmlow, 1980; also see Chapter 9 in this volume). Accommodative (AS) and vergence (VS) stimuli are input to the accommodative (upper loop) and vergence (lower loop) system, respectively. The thresholds for initiating a response are represented by the depth-of-focus and Panum's fusional area, respectively. The proximal input (PS), representing the awareness of nearness, goes through gain elements and is input to the accommodative and vergence controllers, respectively (Hung et al, 1996). The proximal component has been shown to play a relatively greater role under the accommodative open-loop condition, with only a negligible role under the accommodative closed-loop condition which reflects everyday viewing conditions. The accommodative adaptive element "charges up" during near work, resulting in a slow decay, or "discharge", when the accommodative loop is subsequently opened (Hung and Ciuffreda, 1992). It is this "charge/discharge" property of the adaptive element that is responsible for producing nearwork-induced transient myopia (Hung and Ciuffreda, 1999; Ong and Ciuffreda, 1995, 1997). The adaptive element appears to assist the accommodative system during nearwork, such as reading, by maintaining a more sustained near accommodative response level, so that less change in accommodation is needed to return to the near level following very brief viewing at far. This occurs due to the slowed decay of accommodation following prolonged drive of the adaptive component during nearwork (see Chapter 18 of this volume). Therefore, by adapting to a higher accommodative level, less accommodative drive/effort is needed to return to the nearwork response level. However, excessively slowed decay, as seen in symptomatic individuals, may hinder normal accommodative responsivity. The interactive accommodative convergence component, represented by the AC/A ratio, serves to drive the vergence output. Conversely, convergence accommodation, represented by the CA/C ratio, serves to drive the accommodative output. These interactive effects are also discussed in detail in Chapter 9 of this volume. The tonic components represent the bias or "default" response levels in the absence of blur, disparity, or proximal stimulation (Rosenfield et al, 1993, 1994; Hung and Ciuffreda, 1991). Thus, when both systems are rendered open-loop, the systems return to their respective default tonic values. The accommodative plant represents the ciliary muscle/lens complex and provides the output of the accommodation system. The vergence plant represents the extraocular muscles and the eyeball, and it provides the output of the vergence system.

The descriptive model above provides an overview of the detailed comprehensive model of accommodation and vergence developed by Hung

and Ciuffreda (1999) (see Fig. 8.25b). The detailed model consists of two feedback control loops driven by target defocus and binocular disparity, respectively. The two loops are connected via the accommodative convergence (AC) and convergence accommodation (CA) crosslinks. In the accommodative loop, the difference between the accommodative stimulus (AS) and response (AR), or accommodative error (AE) (i.e., retinal defocus), is input to the nonlinear deadspace element (±DSP) representing the DOF. If this input exceeds the DOF, then the output, which is now retinal-image blur, is input to the accommodative controller having gain ACG. The accommodative controller output is summed with tonic accommodation (ABIAS) and the crosslink signal via convergence accommodation to provide the aggregate accommodative response. Also, the accommodative controller output is multiplied by the crosslink gain, AC, to provide the accommodative convergence signal. Similarly, in the vergence loop, the difference between the vergence stimulus (VS) and response (VR), or vergence error (VE) (i.e., retinal disparity), is input to the nonlinear deadspace element (±DSP), representing Panum's fusional area (Panum, 1858). If this input exceeds Panum's fusional area, then the output from the deadspace element is input to the vergence controller having gain VCG. The vergence controller output is summed with tonic vergence (VBIAS) and the crosslink signal via accommodative convergence to provide the aggregate vergence response. Also, the vergence controller output is multiplied by the crosslink gain, CA, to provide the convergence accommodation signal.

In addition to the basic dual-interactive model, the unique feature of this model is the incorporation of both proximal (Hung et al, 1996) and adaptive (Hung, 1992) elements. The input to the proximal component is represented by a distance stimulus (DS), which drives the perceived distance gain (PDG). The output of PDG is input to both the accommodative proximal gain (APG) and vergence proximal gain (VPG) elements, which are summed with the respective controller outputs. It has been shown that while the proximal component constitutes a considerable percentage (up to about 80%) of the accommodative response under open-loop conditions, it provides a negligible contribution (<4%) under normal closed-loop conditions when visual feedback is present (Hung et al, 1996).

The adaptive element in each loop receives its input signal from the controller output, which in turn modifies the time constant of the controller itself. Although this configuration is unique among near-response oculomotor models, the modification of a component's time constant is seen in other systems. For example, in the saccadic system, Optican and Miles (1985) simulated adaptation using modification of time constants. In our model, the accommodative controller output is input to a multiplier, m_A, and compression element, CE, to drive the adaptive element having gain, K_A, and

time constant, T_{A1}. The multiplier and compression elements are necessary to provide a saturation effect for large inputs that is seen in the adaptation experiments (Fisher et al, 1990; Rosenfield and Gilmartin, 1989). The adaptive element output, a, modifies the time constant of the accommodative controller via the term, $T_{A2}+ |a^3|$, where T_{A2} is the fixed portion of the time constant. The cubic relationship was obtained empirically to provide negligible increase in time constant for smaller amounts of adaptation, but a large increase in time constant for larger amounts of adaptation. Similar to the accommodative adaptive element, the vergence adaptive component consists of multiplier, m_V, compression element, CE, adaptive gain, K_V, adaptive time constant, T_{V1}, adaptive element output, b, and controller time constant $T_{V2}+ |b^3|$.

The nominal parameter values are: PDG=0.212, APG=2.1, ACG = 10, AC = 0.80 MA/D, ABIAS = 0.61 D, $m_A = 3$, $T_{A1} = 25$ sec, $T_{A2} = 4$ sec, and VPG=0.067, VCG = 150.0, CA = 0.37 D/MA, VBIAS = 0.29 MA, $m_V = 05$, $T_{V1} = 50$ sec, $T_{V2} = 8$ sec, $K_V = 9$ (Hung, 1992; Hung et al, 1996).

This comprehensive dynamic model has been used to simulate nearwork-induced transient myopia (NITM; Ong and Ciuffreda, 1997) in different refractive groups (Hung and Ciuffreda, 1999a) as well in a model of refractive error development (Hung and Ciuffreda, 1999b; also see Chapter 18 of this volume).

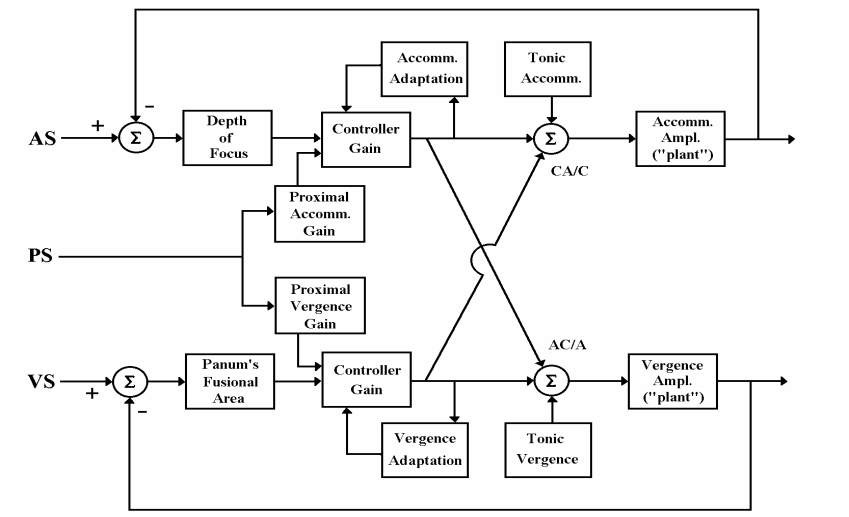

Fig. 8.25a. Hung and Ciuffreda descriptive comprehensive model of the accommodation and vergence system (Hung et al, 1996; Ciuffreda et al, 2000). Reprinted from Ciuffreda et al (2000), pg. 196, Fig. 2, with permission of Birkh←user Verlag.

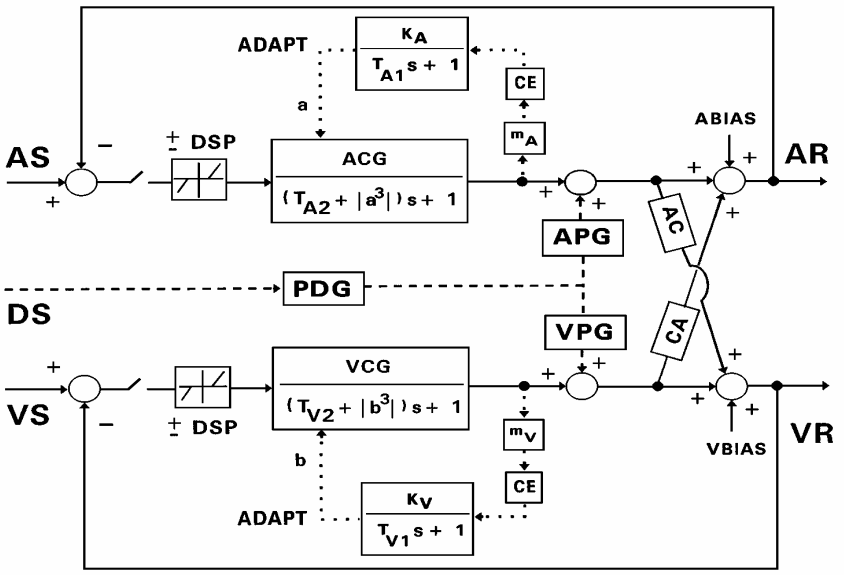

Fig. 8.25b. Hung and Ciuffreda detailed comprehensive model of the accommodation and vergence system (Hung and Ciuffreda, 1999a). Reprinted from Hung and Ciuffreda (1999a), pg. 151, Fig. 1, with permission of Elsevier Science.

8.5 SUMMARY

The basic biomechanical aspects of accommodation were understood nearly 150 years ago (Helmholtz, 1855). Yet, it was not until the introduction of feedback control theory nearly 40 years ago that true quantitative understanding of the accommodative control process began to develop. Proportional control was used to describe the steady-state behavior, but it exhibited nearly instantaneous, or extremely rapid dynamics, since no lag terms were associated with a purely proportional control element. Then, integral control was used to provide smoother dynamic behavior, but it could not simulate steady-state behavior. Later, proportional-integral control was used to attain both dynamic and steady-state behavior, but it had to contend with feedback instability due to the long latency and slow dynamics. More recently, switching control was introduced which restricted the response regions so that accurate simulation was possible. But these models could only be applied under limited conditions, since simulated responses outside of the restricted regions resulted in unrealistic responses. Finally, dual-mode control overcame these difficulties by providing only two

possible modes. The fast open-loop mode operated for fast, large amplitude stimuli. It used rate of change, as well as magnitude, of retinal-image defocus to determine the appropriate direction for the accommodative response. In support of this, Mays and Gamlin (2000) have found velocity signals in the Edinger-Westphal nucleus that could be used by the accommodation system. The fast component thus attained most of the response amplitude and overcame the instability problem associated with a relatively long latency. The slow, closed-loop mode operated for slow and small amplitude stimuli. It further reduced the residual error via proportional control to provide an accurate steady-state response.

Simulations of the dual-mode model have provided answers to the two major problems posed in the beginning of this chapter. First, the accommodation system overcomes the even-error problem by using in part the rate of change of retinal defocus to determine the target direction. Of course, in daily life, other cues such as binocular disparity, vergence innervation, chromatic aberration, spherical aberration, size, perspective, and overlap all assist to provide a relatively robust system for determining target direction. Second, experimental and modeling results support a dual-mode, or discontinous, process for accommodation consisting of a fast open-loop movement followed by slow closed-loop control to reduce the error to a minimum. This explains rather well the pure step responses, and the staircase-like step responses to both ramp and sinusoidal stimuli. However, the pulse responses, which shows durations similar to pulse stimuli and therefore are suggestive of a continuous system, appear to present a problem for a discontinuous model. However, the dual-mode model can account for the pulse response data based on re-triggering during the downward transition of the pulse. Therefore, the overall response has the shape of a pulse with a duration approximately equal to that of the pulse stimulus, and thus resembles that of a simple continuous system, even though the underlying process is discontinuous.

Thus, these models have not only clarified our thought processes regarding the normal control of the accommodation system, but have also provided quantitative solutions to some of the fundamental problems that have perplexed investigators for over a century. Some questions still remain regarding both normal and abnormal control of accommodation. First, what are the key features of a dynamic, combined interactive model of accommodation and vergence that will provide all the normal response characteristics? Second, what static and dynamic model parameters can describe and be responsible for abnormal accommodative conditions, as found in patients with accommodative infacility (Ciuffreda, in press)? Lastly, can normal and abnormal accommodation systems be trained, can model parameters associated with such training be identified, and can

optimal training paradigms be developed based on current and future models? It is clear from what has been achieved up to this point that modeling and simulation of these clinical conditions will continue to play a significant role in resolving clinical problems by providing insight into the underlying mechanisms of accommodative deficits. This will benefit clinicians and vision scientists, as well as bioengineers, by providing a common, clear, and concise language of models in gaining a deeper understanding of the intricate and elegant control process of accommodation.

8.6 REFERENCES

Bahill, A. T. and Stark, L., 1979, The trajectory of saccadic eye movements, *Sci. Am*. **240**: 108-117.

Benjamin, W. J., ed., 1998, *Borish's Clinical Refraction: Principles and Practice*, W. B. Saunders and Co., Philadel., PA.

Brodkey, J. D., and Stark, L., 1967, Accommodative convergence - an adaptive nonlinear system, *IEEE Trans. Sys. Sci. Cyber*. **3**: 121-133.

Campbell, F. W., 1957, The depth of field of the human eye, *Optica Acta*. **4**: 157-164.

Campbell, F. W., 1959, Fluctuations of accommodation under steady viewing conditions, *J. Physiol*. **145**: 579-594.

Campbell, F. W., and Westheimer, G., 1960, Dynamics of the accommodation responses of the human eye, *J. Physiol*. **151**: 285-295.

Chauhan, K., and Charman, W. N., 1995, Single figure indices for the steady-state accommodative response, *Ophthal. Physiol. Opt*. **15**: 217-221.

Ciuffreda, K. J., 1991, Accommodation and its anomalies, in: *Vision and Visual Dysfunction: Visual Optics and Instrumentation, vol. 1*, W. N. Charman, ed., Macmillan, London, pp. 231-279.

Ciuffreda, K. J., 1998, Accommodation, pupil, and presbyopia, in: *Borish's Clinical Refraction: Principles and Practice*, W. J. Benjamin, ed., W. B Saunders, Philadel., PA, pp. 77-120.

Ciuffreda, K.J., Scientific basis for and efficacy of optometric vision therapy in non-strabismic vergence and accommodative dysfunction, *Optometry*, in press.

Ciuffreda, K. J., Hokoda, S. C., Hung, G. K., and Semmlow, J. L., 1984, Accommodative stimulus/response function in human amblyopia, *Doc. Ophthalmol.* **56**: 303-326.

Ciuffreda, K. J., and Kenyon, R. V., 1983, Accommodative vergence and accommodation in normals, amblyopes, and strabismics, in: *Vergence Eye Movements: Basic and Clinical Aspects*, C. M. Schor, and K. J. Ciuffreda, eds., Butterworths, Boston, pp. 101-173.

Ciuffreda, K. J., and Kruger, P. B., 1988, Dynamics of human voluntary accommodation, *Am. J. Optom. Physiol. Opt*. **65**: 365-370.

Ciuffreda, K. J., Levi, D. M., and Selenow, A., 1991, *Amblyopia: Basic and Clinical Aspects*. Butterworths, Boston, MA.

Ciuffreda, K. J., Rosenfield, M., and Chen, H.-W., 1997, The AC/A ratio, age, and presbyopia, *Ophthal. Physiol. Opt*. **17:** 307-315.

Ciuffreda, K. J., Rosenfield, M., and Chen, H. W., 2000, Accommodation, age, and presbyopia, in: *Accommodation and Vergence Mechanisms in the Visual System*, O. Franzén, H. Richter, and L. Stark, eds., Birkhäuser Verlag, Basel, Switzerland, pp. 193-200.

Ciuffreda, K. J., and Rumpf, D., 1985, Contrast and accommodation in amblyopia, *Vis. Re*s. **25**: 1445-1457.

D'Azzo, J. D., and Houpis, C. H., 1988, *Linear Control System Analysis and Design, Conventional and Modern*, McGraw Hill, New York, pp. 209-251.

Fincham, E. F., 1951, The accommodation reflex and its stimulus, *Br. J. Ophthalmol*. **35**: 381-393.

Fisher, S. K., and Ciuffreda, K. J., and Bird, J. E., 1990, The effect of stimulus duration on tonic accommodation and tonic vergence, *Optom. Vis. Sci.* **67**: 441-449.

Fujii, K., Kondo, K., and Kasai, T., 1970, An analysis of the human eye accommodation system*, Osaka Univ. Tech. Report No. 925, Vol. 20*, pp. 221-236.

Gamlin, P. D. R., 1999, Subcortical neural circuits for ocular accommodation and vergence in primates, *Ophthal. Physiol. Opt*. **19**: 81-89.

Gilmartin, B., and Hogan, R. E., 1985, The relationship between tonic accommodation and ciliary muscle innervation, *Invest. Ophthal. Vis. Sci*. **26**: 1024-1028.

Gray, L. S., Winn, B., and Gilmartin, B., 1993, Accommodative fluctuations and pupil diameter, *Vis. Res*. **33**: 2083-2090.

Harrison, R. J., 1987, Loss of fusional vergence with partial loss of accommodative convergence and accommodation following head injury, *Bino. Vis*. **2**: 93-100.

Heath, G. G., 1956a, Components of accommodation, *Am. J. Optom. Arch. Am. Acad. Optom*. **33**: 569-579.

Heath, G. G., 1956b, The influence of visual acuity on accommodative responses of the eye, *Am. J. Optom. Arch. Am. Acad. Optom*. **33**: 513-524.

Helmholtz, H., 1855, Uber die Accommodation des Auges, *Albrecht v. Graefes Arch. Ophthal*. **1**: 1-74.

Hess, C., 1904, Observations concerning accommodation organs, *Klin. Mbl. Augenheilk*., **42**: 309-315.

Hokoda, S. C., and Ciuffreda, K. J., 1983, Theoretical and clinical importance of proximal vergence and accommodation, in: *Vergence Eye Movements: Basic and Clinical Aspects*, C. M. Schor, and K. J. Ciuffreda, eds., Butterworths, Boston, pp. 75-97.

Hung, G. K., 1998, Sensitivitiy analysis of the stimulus/response function of a static nonlinear accommodation model, *IEEE Trans. Biomed. Engin*. **45**: 335-341.

Hung, G. K., 1992, Adaptation model of accommodation and vergence, *Ophthal. Physiol. Opt.,* **12**: 319-326.

Hung, G. K., 1997, Quantitative analysis of the accommodative convergence to accommodation ratio: linear and nonlinear static models, *IEEE Trans. Biomed. Engin.,* **44**: 306-316.

Hung, G. K., 1998, Dynamic model of the vergence eye movement system: simulation using MATLAB/SIMULINK, *Comp. Meth. Prog. Biomed*. **55**: 59-68.

Hung, G. K., Semmlow, J. L., and Ciuffreda, K. J., 1986, A dual-mode dynamic model of the vergence eye movement system, *IEEE Trans. Biomed. Engin*. **33**: 1021-1028.

Hung , G. K., and Ciuffreda, K. J., 1988, Dual-mode behaviour in the human accommodation system, *Ophthal. Physiol. Opt*. **8**: 327-332.

Hung, G. K., and Ciuffreda, K. J., 1991, Model of accommodation after sustained near focus, *Optom. Vis. Sci.*, **68**: 617-623.

Hung, G. K., and Ciuffreda, K. J., 1999a, Adaptation model of nearwork-induced transient myopia, *Ophthal. Physiol. Opt*. **19**: 151-158.

Hung, G. K., and Ciuffreda, K. J., 1999b, Model of human refractive error development, *Curr. Eye Res*. **19**: 41-52.

Hung, G., K., Ciuffreda, K. J., and Rosenfield, M., 1996, Proximal contribution to a linear static model of accommodation and vergence, *Ophthal. Physiol. Opt*. **16**: 31-41.

Hung, G. K., Ciuffreda, K. J., Semmlow, J. L., and Hokoda, S. C., 1983, Model of static accommodative behavior in human amblyopia, *IEEE Trans. Biomed. Engin*. **30:** 665-672.

Hung , G. K. and Semmlow , J. L. , 1980, Static behavior of accommodation and vergence : computer simulation of an interactive dual-feedback system, *IEEE. Trans. Biomed. Eng.* **27**: 439-447.

Hung, G. K., Semmlow, J. L., and Ciuffreda, K. J., 1982, Accommodative oscillation can enhance average accommodative response: a simulation study**,** *IEEE Trans. Sys. Man Cyber*. **12**: 594-598.

Hung, G. K., Semmlow, J. L., and Ciuffreda, K. J., 1986, A dual-mode dynamic model of the vergence eye movement system, *IEEE Trans. Biomed. Engin.* **33**: 1021-1028.

Jampel, R. S., 1959, Representation of the near-response on the cerebral cortex of the macaque, *Am. J. Ophthal*. **48**: 573-582.

Jiang, B.-C., 2000, A modified control model for steady-state accommodation, in: *Accommodation and Vergence Mechanisms in the Visual System*, O. Franzén, H. Richter, and L. Stark, eds., Birkhäuser Verlag, Basel, Switzerland, pp. 235-243.

Johnson, C. A., 1976, Effects of luminance and stimulus distance on accommodation and visual resolution, *J. Opt. Soc. Am*. **66**: 138-142.

Kasai T., Unno, M., Fujii. K., Sekiguchi, M., Shinohara, K., 1971, Dynamic characteristics of human eye accommodation system, *Osaka Univ. Tech. Report, Vol. 21*, pg. 569.

Kaufman, P. L., 1992, Accommodation and presbyopia. Neuromuscular and biophysical aspects, in: Adleer's Physiology of the Eye, 9th Ed., W. M. Hart, ed., Mosby-Year Book, St. Louis, MO., pg. 397.

Krall, A. M., and Fornaro, R., 1967, An algorithm for generating root locus diagrams, *Commun. of the Assoc. on Computing Machinery*. **10**: 186-188.

Khosroyani, M., 2000, *Computer Simulation of Ocular Accommodation and Vergence Models.* M. S. Thesis. Tarbiat Modarres University, Tehran, Iran.

Krishnan , V. V. , and Stark , L., 1975, Integral control in accommodation, *Comp. Prog. Biomed*. **4**: 237-255.

Liebowitz, H. W., and Owens, D. S., 1978, New evidence for the intermediate position of relaxed accommodation, *Doc. Ophthalmol*. **46**: 133-147.

Mays, L. E., and Gamlin, P. D. R., 2000, Neuronal circuits for accommodation and vergence in primates, in: *Accommodation and Vergence Mechanisms in the Visual System*, O. Franzén, H. Richter, and L. Stark, eds., Birkhäuser Verlag, Basel, Switzerland, pp. 1-9.

Mordi, J. A., and Ciuffreda, K. J., 1998, Static aspects of accommodation: age and presbyopia, *Vis. Res*. **38**: 1643-1653.

Morgan, M. W., 1957, The resting state of accommodation, *Am. J. Optom. Arch. Am. Acad. Optom*. **34**: 347-353.

Morgan, M. W., 1968, Accommodation and vergence, *Am. J. Optom. Arch. Am. Acad. Optom.* **45**: 417-454.

Moses, R. A., ed., 1981, *Adler's Physiology of the Eye, Clinical Applications*, C. V. Mosby Co., St. Louis, pp 440-455.

Neveu, C., and Stark, L., 1995, Hysteresis in accommodation, *Ophthal. Physiol. Opt*. **15**: 207-216.

Ohtsuka, K., Maekawa, H., Takeda, M., Uede, N., and Chiba, S., 1988, Accommodation and convergence insufficiency with left middle cerebral artery occlusion, *Am. J. Ophthalmol.* **105**: 60-64.

O'Neill, W. D., 1969, An interactive control systems analysis of the human lens accommodative controller, *Automatica*. **5**: 645-654.

Ong, E., and Ciuffreda, K. J., 1995, Nearwork-induced transient myopia - a critical review, *Doc. Ophthalmol*. **91**: 57-85.

Ong, E., and Ciuffreda, K. J., 1997, *Accommodation, Nearwork, and Myopia*, Optometric Extension Program Foundation, Inc., Santa Ana, CA.

Optican, L M., and Miles, F. A., 1985, Visually induced adaptive changes in primate saccadic oculomotor control signals, *J. Neurophysiol*. **54**: 940-958.

Panum, P. L, 1858, *Physiologische Untersuchungen uber das Sehen mit zwei Augen, Schwersche Buchhandlung*, Kiel, Germany.

Phillips, S. R., 1974, *Ocular Neurological Control Systems: Accommodation and the Near Response Triad*, Ph.D. Dissertation, Dept. of Mechanical Engin., Univ. of Calif., Berkeley, CA, U.S.A.

Provine, R. R., and Enoch, J. M., 1975, On voluntary ocular accommodation, *Percept. Psychophys*. **17**: 209-212.

Ripps, H., Chin, N. B., Siegel, I. M., and Breinin, G. M., 1962, The effect of pupil size on accommodation, convergence, and the AC/A ratio, *Invest. Ophthal. Vis. Sci*. **1**: 127-135.

Rosenfield, M., Ciuffreda, K. J., Hung, G. K., 1991, The linearity of proximally induced accommodation and vergence, *Invest. Ophthal. Vis. Sci*. **32**: 2985-2991.

Rosenfield, M., Ciuffreda, K. J., Hung, G. K., and Gilmartin, B., 1993, Tonic accommodation: a review. I. Basic aspects, *Ophthal. Physiol. Opt*. **13**: 266-284.

Rosenfield, M., Ciuffreda, K. J., Hung, G. K., and Gilmartin, B., 1994, Tonic accommodation: a review. II. Accommodative adaptation and clinical aspects, *Ophthal. Physiol. Opt*. **14**: 265-277.

Rosenfield, M., and Gilmartin, B., 1989, Temporal aspects of accommodative adaptation, *Optom. Vis. Sci*. **66**: 229-234.

Saladin, J. J. and Stark, L., 1975, Presbyopia: a new evidence from impedance cyclography supporting the Hess-Gullstrand theory, *Vis. Res*. **15**: 537-541.

Stark, L., 1987, Presbyopia in light of accommodation, in *Presbyopia, Recent Research and Reviews from the Third International Symposium*, L. Stark, and G. Obrecht, eds, Professional Press, New York, pp. 264-274.

Stark, L., Kong., R., Schwartz, S., and Hendry, D., 1976, Saccadic suppression of image displacement, *Vis. Res*. **16**: 1185-1187.

Stark, L. W., Neveu, C. and Krishnan, V. V., 2000, Mode switching in control of accommodation, in: *Accommodation and Vergence Mechanisms in the Visual System*, O. Franzén, H. Richter, and L. Stark, eds., Birkhäuser Verlag, Basel, Switzerland, pp. 225-234.

Stark, L., and Takahashi, Y., 1962, Accommodative tracking, *Quart. Prog. Rept., Res. Lab. of Electronics, M.I.T.* **67**: 220.

Stark, L., Takahashi, Y., and Zames, G. 1962, The dynamics of the human lens system, *Quart. Prog. Rept., Res. Lab. of Electronics, MIT*. **66**: 337.

Stark, L., Takahashi, Y., and Zames, G. 1965. Nonlinear servo-analysis of human lens accommodation. *IEEE Trans. Sys. Sci. Cyber*. **1**: 75-83.

Sun, F., and Stark, L., 1990, Switching control of accommodation: experimental and simulation responses to ramp inputs, *IEEE Trans. Biomed. Engin*. **37**: 73-79.

Thompson, H. E., 1975, *The Dynamics of Accommodation in Primates*, Ph.D. dissertation, Dept. of Biomed. Engin., Univ. of Illinois Medical Center, Chicago, IL.

Toates, F. M., 1972a, Accommodation function of the human eye, *Physiol. Reviews*. **52**: 828-863.

Toates, F. M., 1972b, Studies on the control of accommodation and convergence, *Measurement and Control*. **5**: 58:61.

Tucker, J., and Charman, W. N., Reaction and response times for accommodation, *Am. J. Optom. Physiol. Opt*. **56**: 490-503.

Warwick, R., 1954, The ocular parasympathetic nerve supply and its mesencenphalic sources, *J. Anat., Lond*. **88**: 71-93.

Westheimer, G., 1963, Amphetamines, barbiturates and accommodative convergence, *Arch. Ophthalmol*. **70**: 830-836.

Winn, B., Pugh, J. R., Gilmartin, B., and Owens, H., 1990, Arterial pulse modulates steady-state ocular accommodation, *Curr. Eye Res*. **9**: 971-974.